

**MEASURING PARITY VIOLATION
IN COBALT-60 DECAY**

By

Paul R. Lashomb

A thesis submitted in partial fulfillment of the
Requirements for the degree of

Bachelor of Science

Houghton College

November 12, 2015

Signature of Author.....

Department of Physics
November 12, 2015

.....

Dr. Mark Yuly
Professor of Physics
Research Supervisor

.....

Dr. Brandon Hoffman
Associate Professor of Physics

**MEASURING PARITY
VIOLATION IN COBALT-60
DECAY**

By

Paul R. Lashomb

Submitted to the Department of Physics
on November 12, 2015 in partial fulfillment of the
requirement for the degree of
Bachelor of Science

Abstract

An experiment was performed to measure parity violation in the decay of ^{60}Co . Measurements of the correlation between the circular polarization of γ -rays and β -particles were made by measuring the circular polarization of the decay γ -ray emitted at 180° from the correlated β -particle. A γ - β coincidence circuit counted gamma rays transmitted through a magnetized iron core. Since the Compton scattering cross-section for circularly polarized γ -rays depends on the spin orientation of the electrons in the magnet, an asymmetry in the count rate when the electron and photon spins are parallel and anti-parallel indicates parity violation. While only initial measurements have been made to date, in the future it should be possible to measure the asymmetry to within approximately 5%.

Thesis Supervisor: Dr. Mark Yuly
Title: Professor of Physics

TABLE OF CONTENTS

| | |
|------------------------------------------------------------------------------------------|-----------|
| Chapter 1: Introduction..... | 5 |
| 1.1 Parity..... | 5 |
| 1.2 History..... | 6 |
| 1.2.1 Parity in the 20 th Century..... | 6 |
| 1.2.2 Beta Decay..... | 7 |
| 1.3 Lee and Yang's Paper..... | 10 |
| 1.4 The Wu Experiment..... | 12 |
| 1.4.1 Test for Parity Conservation in Beta Decay..... | 12 |
| 1.4.2 Measurements that Would Indicate a Violation of Parity..... | 14 |
| 1.4.3 Results of the Wu Experiment..... | 15 |
| 1.4.4 The Violation of Parity..... | 17 |
| 1.5 Testing for Conservation of Parity..... | 17 |
| Chapter 2: Theory..... | 21 |
| 2.1 Spin, Polarization, and Momentum Conservation..... | 21 |
| 2.2 Helicity..... | 24 |
| 2.3 Indicator of Parity Violation..... | 25 |
| 2.4 Calculations of Count Rate Estimates..... | 27 |
| 2.4.1 Measurement of Circular Polarization of Gamma Rays..... | 27 |
| 2.4.2 Cross-section Calculations..... | 29 |
| 2.4.3 Correlation between Circularly Polarized γ -Rays and β Particles..... | 30 |
| Chapter 3: Experiment..... | 36 |
| 3.1 Description of Apparatus..... | 36 |
| 3.2 Electronics..... | 45 |
| 3.3 TAC Output and Calibration..... | 47 |
| 3.4 Analysis..... | 48 |
| 3.5 Experimental Difficulties..... | 49 |
| Chapter 4: Results and Conclusion..... | 50 |
| 4.1 Discussion..... | 50 |
| 4.2 Conclusion and Future Plans..... | 50 |

TABLE OF FIGURES

| | |
|-----------------------------------------------------------------------------------------------------------------|----|
| Figure 1. A ^{60}Co nucleus oriented in +z direction..... | 5 |
| Figure 2. Feynman diagram of beta decay..... | 8 |
| Figure 3. Electron energy spectrum..... | 9 |
| Figure 4. Wu experiment apparatus..... | 13 |
| Figure 5. ^{60}Co decay and mirror decay..... | 14 |
| Figure 6. Wu experiment γ -ray and electron asymmetry..... | 16 |
| Figure 7. Transmission of γ -rays through electromagnet if parity symmetry conserved..... | 18 |
| Figure 8. Transmission of γ -rays through electromagnet if parity symmetry not conserved..... | 19 |
| Figure 9. Decay scheme of ^{60}Co | 22 |
| Figure 10. Conservation of angular momentum..... | 23 |
| Figure 11. Helicity of neutrino to noninterial and interial observers..... | 25 |
| Figure 12. Decay and mirror decay of ^{60}Co with circularly polarized γ -rays..... | 26 |
| Figure 13. Compton scattering from polarized electrons..... | 28 |
| Figure 14. Transmission of circularly polarized γ -rays through electromagnet | 30 |
| Figure 15. Estimated asymmetry in γ -ray transmission as a function of thickness..... | 32 |
| Figure 16. Estimated asymmetry in γ -ray transmission as a function of initial γ -ray energy..... | 33 |
| Figure 17. Estimated asymmetry in γ -ray transmission as a function of collection time..... | 34 |
| Figure 18. Estimated relative uncertainty in count rate as a function of collection time..... | 35 |
| Figure 19. Diagram of constructed apparatus..... | 37 |
| Figure 20. Photograph of electromagnet and detectors..... | 38 |
| Figure 21. Photograph of bottom acrylic mount for electromagnet..... | 39 |
| Figure 22. Photograph of top view of acrylic mount..... | 40 |
| Figure 23. Cross-sectional diagram of top acrylic mount..... | 40 |
| Figure 24. Photograph of ^{60}Co source..... | 41 |
| Figure 25. Photograph of entire apparatus used..... | 42 |
| Figure 26. Electromagnet saturation without steel plate..... | 43 |
| Figure 27. Electromagnet saturation with 6.223 mm steel plate..... | 43 |
| Figure 28. Electromagnet saturation with 10.0 mm steel plate..... | 44 |
| Figure 29. Fast-timing NIM circuit diagram..... | 45 |
| Figure 30. Histogram of timing spectrum from TAC output..... | 47 |
| Figure 31. Histogram of γ -ray energy spectrum from MCA output..... | 48 |

1.1 Parity

In nature, physical symmetries can be utilized in order to more easily explain the behavior of the world around us. Systems that may seem, at first, to be rather complicated can be greatly simplified if their symmetries are sufficiently understood.

One particular symmetry that has been observed in the electromagnetic, strong, and gravitational force is invariance under a parity transformation. A parity transformation is the inversion of the spatial coordinate axes. An interaction that is invariant under this transformation is parity symmetric. A related transformation is reflection (i.e., the mirror). The reflection transformation is identical to a parity transformation followed by a rotation. Both the parity and reflection transformations result in a right-handed coordinate system changing into a left-handed coordinate system. As an example of the reflection transformation, consider the polarized ^{60}Co nucleus oriented in the $+z$ direction in Figure 1. After a reflection transformation, the spin of the nucleus will point in the $-z$ direction.

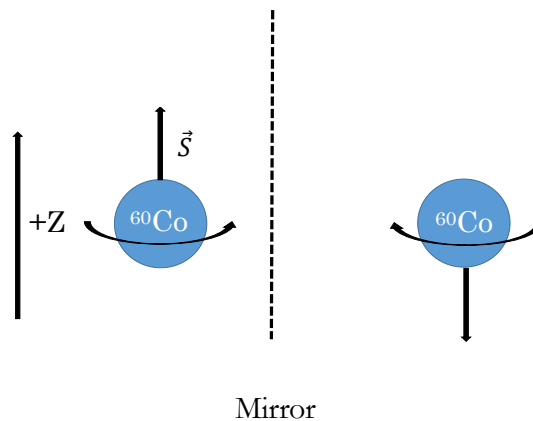


Figure 1: A ^{60}Co nucleus polarized in the $+z$ direction. In the mirror, the spin of ^{60}Co nucleus reverses its orientation and points in the $-z$ direction.

An invariance under the reflection transformation means that a measurement in the right-handed and left-handed system will yield the same result after the interaction. In other words, if a measurement is made of an interaction that is parity symmetric, then the measurement will be unaffected by the parity transformation of that space.

As an example, consider a system governed by the gravitational interaction. The system and its mirror image are indistinguishable and, thus, the interaction is invariant under a reflection transformation. Because it is invariant under a reflection transformation, then measurements made in the right-handed coordinate system yield the same value as measurements made in the mirror-image, left-handed coordinate system. Interactions that exhibit parity symmetry are parity conserving. In contrast, if parity symmetry was violated, for instance hypothetically in the gravitational interaction, then a measurement of the gravitational forces between two objects would yield different values for the system and its mirror image.

The purpose of the experiment described in this thesis was to test whether parity is conserved in the weak interaction by using the ^{60}Co beta decay process. Particles have their own handedness which is indicated by their helicity. For a right-handed particle, its momentum and spin are parallel and for a left-handed, they're anti-parallel. By measuring emitted γ -rays and β -particles in coincidence at 180° relative each other's direction of emission, an asymmetry in the emission of left-handed and right-handed polarized photons is an indication of the violation of parity symmetry or, simply, parity violation.

1.2 History

1.2.1 Parity in the 20th Century

The overwhelming evidence for parity conservation in physical interactions, with the exception of the weak force, led physicists of the early 20th century to assume that parity was conserved in the weak interactions as well [1]. When Lee and Yang proposed [2] that parity was not conserved in weak interaction, Richard Feynman, a notable theoretical physicist who received a Nobel prize for his work

in Quantum Electrodynamics, placed a wager of \$50 with a friend that parity in the weak interaction would be conserved, saying, “I thought the idea [of parity violation] unlikely, but possible, and a very exciting possibility” [3]. He would later lose the bet after parity violation was confirmed by experiment.

Wolfgang Pauli, for whom the “Pauli Exclusion Principle” is named and who also theorized the existence of the neutrino, upon being informed that parity in the weak interaction was not conserved, was reported to have commented, “That’s total nonsense!” and, upon being reassured that it was verified, exclaimed, “Then, it must be repeated!”[4].

On a more humorous note, Pauli wrote as a condolatory notice in an addendum to the letter of 29 January 1957 to Markus Fierz, an assistant of Pauli’s, “It is our sad duty to make known that our dear friend PARITY gently passed away on 19 January 1957 after a short suffering under further experimental interference. In the name of the survivors, e, μ, ν' .” [5]

Clearly, physicists were confident that parity was conserved in the weak interaction and the idea of parity violation was radical at that time.

1.2.2 Beta Decay

In order to test for parity symmetry in the weak interaction, β -decay can be utilized as it is governed by the weak force. The nuclear beta decay process is the most common weak interaction process, making it suitable for measurements of parity conservation. In order to discuss the role of β -decay in tests for conservation of parity, it is necessary to first introduce the theory of beta decay. Beta decay is a nuclear decay process in which a parent nucleus decays into a daughter nucleus by the emission of a β^\pm particle that is, an electron or positron, respectively, and a neutrino or anti-neutrino. Specifically, β^- , which is of particular interest to the experiment outlined in this thesis, decays by the following:

$${}^A_Z P \rightarrow {}^A_{Z+1} D + e^- + \bar{\nu}_e, \quad (1)$$

where P is the parent nucleus and D is the daughter nucleus. Note that the daughter has $Z + 1$ protons. This occurs by the neutron decay, within the nucleus,

$$n \rightarrow p + e^- + \bar{\nu}_e, \quad (2)$$

which maintains the total number of nucleons, A, while increasing the number of protons.

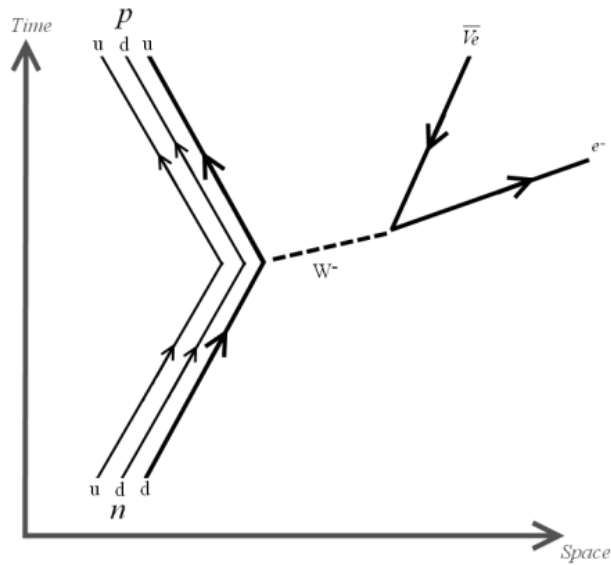


Figure 2: Feynman diagram of beta decay. By convention, anti-particles, like the anti-neutrino, travel backwards in time. Figure taken from Ref [21].

The neutron, which is made up of constituent particles called quarks, changes from a quark content of (u, d, d) to (u, u, d) , which is the quark content of a proton. It does so by the emission of a W^- boson which then decays,

$$W^- \rightarrow e^- + \bar{\nu}_e . \quad (3)$$

Figure 2 is a Feynman diagram that gives a pictorial representation of the β^- decay process.

Beta decay was first thought to have the following decay process,



following experiments by Rutherford and Soddy [6] at the beginning of the 1900's which had shown that, what Rutherford had called transmutation, resulted in the conversion of an atom to another atom and emission of a beta particle in the process. Soddy and Fajans found that the resulting atom after this transmutation is to the right on the periodic table of the original atom [7]. Measurements of the energy of β -particles, as can be seen by Figure 3, determined that the energy distribution of β -particles was a continuous distribution curve.

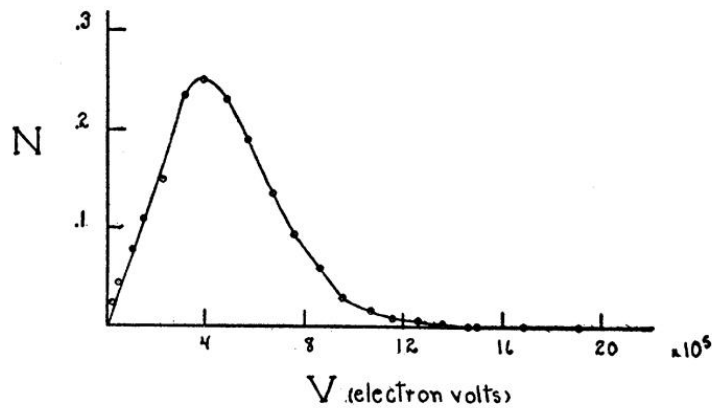


Figure 3: Energy distribution curve of beta rays from Radium E as measured by Scott. Figure taken from Ref [10].

This, however, appears to be a violation of energy conservation. Because the electron's energy followed a distribution, the energy of the emitted electron and the daughter product would not always sum to the total energy of the parent nucleus which is a necessity by energy conservation. Measurements made by Ellis [9], solidified the notion that the β -particle's energy was a continuous spectrum. In Figure 3 is the beta energy spectrum for beta rays emitted from Radium E, as measured by Scott [10].

As can be seen in Figure 3, there is a distribution of emitted beta ray energies from the radioactive source. Since there is an energy distribution rather than a unique energy possessed by the beta rays, Wolfgang Pauli proposed [11] that there must exist another particle in the decay, the neutrino, which shared energy with the electron. In other words, the three bodies in the final state together have zero total momentum and share the energy released in the reaction. Thus, the decay becomes,



where $\bar{\nu}_e$ denotes the anti-neutrino.

This new particle that Wolfgang Pauli had named the “neutron” later would be renamed the “neutrino” by Enrico Fermi in an unpublished private letter to F. Reines in 1952 [12]. In 1956, the first detection of the neutrino [13] was made by F. Reines and C. L. Cowan Jr., confirming the existence of the neutrino. Measurements of the helicity of neutrinos were performed by Goldhaber, *et al.* [14] which determined that the neutrinos are *left-handed*, a result of parity violation in the weak interaction.

1.3 Lee and Yang's Paper

The decay of the θ^+ ($\equiv K_{\pi 2}^+$) and τ^+ ($\equiv K_{\pi 3}^+$) charged strange mesons led to the re-examination of the conservation of parity in weak interactions that, for the electromagnetic, gravitational, and strong force interactions, [1] was well established. The θ^+ and τ^+ decay via the weak interaction into the following:

$$\theta^+ \rightarrow \pi^+ + \pi^0 \quad \text{and}$$

$$\tau^+ \rightarrow \pi^+ + \pi^+ + \pi^-.$$

The θ^+ and τ^+ were experimentally determined to have identical masses and lifetimes even as the accuracy of experimental measurements increased indicating they may be the same particle. [2] Contrary to this, angular momentum and parity conservation suggest that the τ^+ and the θ^+ are different particles. The decay products of the θ^+ and τ^+ have different angular momenta and opposite parities indicating that the τ^+ and the θ^+ are different particles. This was known as the $\tau - \theta$ puzzle. This dilemma was the motivation behind Lee and Yang's work, leading to the suggestion of parity violation. Lee and Yang had claimed that experimental data was insufficient, at the time, to make any conclusive assertions on whether parity was conserved in weak interactions. They proposed three individual experiments that could be performed to directly test for conservation of parity in the weak interaction. The first was carried out by Chien-Shiung Wu [15] using the decay of ^{60}Co . This experiment measured the β radiation from a polarized radioactive source to determine if an asymmetry existed between the number of β particles emitted parallel and anti-parallel the spin of the parent ^{60}Co nuclei. A difference in the number of electrons emitted parallel and anti-parallel the spin of the parent ^{60}Co nuclei indicated a preferred handedness of the electron. In 1957, Wu detected [15] such an asymmetry in the emission of β particles which was evidence of the violation of parity, in agreement with the prediction of Lee and Yang [2].

The second experiment proposed by Lee and Yang [2] involved the decay of π^+ and was performed by Garwin et. al. [16] after that same year. If parity symmetry is assumed to be violated in the weak interaction, then the μ^+ emitted in the π^+ decay is preferentially polarized with a particular helicity, from the pion's rest frame. By measuring the angular distribution of the muons emitted parallel and anti-parallel the parent π^+ in the muon decay, an asymmetry in their helicities would be an indication of parity violation. In order to detect the spin orientation of the muon, positrons of each helicity were measured relative the spin orientation of the muon, similar to the Wu experiment in measuring the electrons of each helicity relative to the nuclear spin of the ^{60}Co . An asymmetry in this positron emission was detected by Garwin et. al. [16], again demonstrating parity violation in agreement with Wu's results.

The third experiment, an experiment believed impossible by Lee and Yang [2], was performed by 1957 by Schopper et. al. [17] confirming the violation of parity symmetry, in agreement with the prior two experiments performed by Wu et. al. [15] and Garwin et. al. [16]. Rather than measuring the distribution of β -particles in nuclear decay, γ -ray helicity was measured using Compton scattering of circularly polarized γ -rays from the aligned electrons in an electromagnet. If an asymmetry in the number of γ -rays scattered by the electromagnet is observed, then an asymmetry in the number of γ -rays produced by the ^{60}Ni , indicating parity violation. This experiment is similar the experiment that was performed, outlined in this thesis. Rather than testing for an asymmetry in the number of scattered γ -rays through an electromagnet, the experiment outlined in this thesis tests for an asymmetry in the number of circularly polarized γ -rays that are transmitted through an electromagnet. The γ -rays were counted in coincidence with β -particles emitted at 180° relative the γ -rays.

1.4 The Wu Experiment

1.4.1 Test for Parity Conservation in Beta Decay

The experiment performed by Wu [15] measured an asymmetry in the distribution of emission of the β between θ and $\pi-\theta$, where θ is the angle between the electron momentum and the spin axis of the nucleus. Non-zero asymmetry would provide a direct verification of the violation of parity in the weak interaction. The source was a cerium magnesium nitrate crystal containing a thin surface layer of ^{60}Co .

The temperature of the source was lowered using magnets in order to polarize the ^{60}Co specimen using adiabatic demagnetization by way of the Rose-Gorter method [18]. When the temperature of ^{60}Co nuclei was lowered, a magnetic field was applied to the electrons surrounding the nuclei and the electrons, then, exerted a force on the nuclei polarizing the nuclei. An anthracene crystal was used in order to detect the β particles emitted from the ^{60}Co nuclei.

The crystal scintillates and, after traveling through the Lucite rod, light was detected at the end of the rod using a photomultiplier tube not shown in Figure 4.

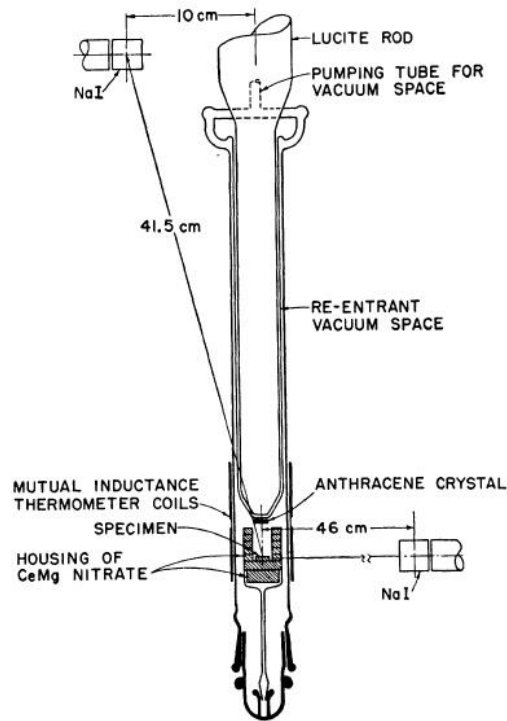


Figure 4: Diagram of the lower part of the cryostat used in the Wu experiment. Electrons emitted from the source anthracene crystal giving off a flash that was sent through the Lucite rod where the light was collected by a photomultiplier tube, not shown in this figure. Two photomultiplier tubes, an equatorial and polar counter positioned 46 cm and 41.5 cm from the source, respectively, monitored the polarity of the source. Electrons were measured when the source was polarized parallel and anti-parallel the length of the vacuum space. Figure taken from Ref [15].

Two additional NaI scintillation detectors were used to monitor the γ -ray anisotropy of the emitted γ -rays from de-excitation of ^{60}Ni , the daughter nucleus of ^{60}Co . The two photomultiplier tubes used for measurement of the γ -ray anisotropy were placed along and perpendicular to the nuclear spin to measure the distribution of γ -rays parallel and perpendicular the nuclear spin.

1.4.2 Measurements that Would Indicate a Violation of Parity

In order to test for the violation of parity, C. S. Wu measured [15] the β -particles emitted parallel and anti-parallel the spin of the ^{60}Co nuclei.

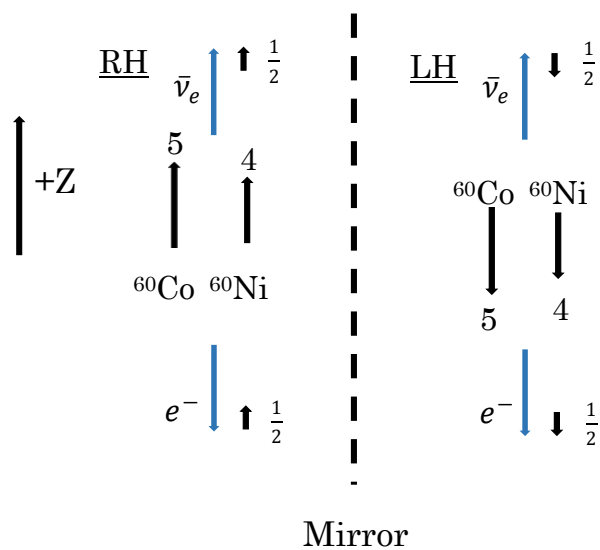


Figure 5: Decay of ^{60}Co and the mirror of the decay. Because the ^{60}Co nuclei possess spin of 5, then the daughter nucleus, ^{60}Ni will carry off a spin of 4 and the electron and anti-neutrino will carry away a spin of $\frac{1}{2}$ each, in order to conserve angular momentum. From the direction of emission and spin of the electron, the electron will be left-handed while, in the mirror of the same decay, its handedness is reversed.

As shown in Figure 5, in order to conserve angular momentum, the total spin of the ^{60}Ni and the emitted β -particle and anti-neutrino must sum to the spin of the ^{60}Co . The β -particles emitted in the $-z$ direction will be left-handed while in the mirror they will be right-handed, by their helicity. The ^{60}Co nuclei were polarized in the $+z$ and the β -particles, now left-handed, were counted. Likewise, the ^{60}Co was also polarized in the $-z$ direction and the β -particles, now right-handed, were counted. Polarizing the ^{60}Co source is equivalent to the system under parity transformation. If a difference in the count-rate of left-handed and right-handed β -particles is observed, then the decay shown on the left in Figure 5 is distinguishable from its mirror and the weak interaction violates parity.

1.4.3 Results of the Wu Experiment

The data collected by Wu, shown in Figure 6 consists of the γ -rays incident the two photomultiplier tubes to determine the polarization of the source using the γ -ray anisotropy and also the number of β -particles measured when the source is polarized parallel and anti-parallel to the β detector in Figure 4. The top plot in Figure 6 is the count rate of the equatorial and polar counters *vs* time. The difference in the count rate of the γ -rays emitted parallel and perpendicular the length of the vacuum space ensures that the ^{60}Co specimen was, in fact, polarized as the theoretical distribution for γ -ray emission from a polarized source predicts a higher intensity of γ -rays perpendicular the spin of the nucleus than parallel the spin which is seen in the plot in Figure 4. The count rates of both detectors approach approximately the same count rate due to the randomization of the emission of γ -rays due to the specimen warming back to room temperature after approximately eight minutes, losing its polarization.

The measurements made of the β -particles is shown in the bottom plot in Figure 6. The plot is of the β count rate *vs* time. Note that, before approximately eight minutes, two separate count rates exist for the β emission. The upper curve is the count rate of β -particles when the ^{60}Co nuclei are polarized at 180° relative the emission direction of the β -particles while the lower curve is the count rate when the ^{60}Co nuclei are polarized parallel the direction of β emission.

As the source warms to room temperature, the asymmetry in the β -particle count rates decreases and disappears at approximately the same time that the polarization of the source disappears. When the ^{60}Co nuclei were polarized 180° relative the β emission direction, a higher count rate of β -particles were observed. The spin direction for the β -particles is the same as the spin of the ^{60}Co nuclei, by conservation of angular momentum. This indicates that a higher number of β -particles with spin opposite their direction of motion were measured than those with spin parallel their direction of motion.

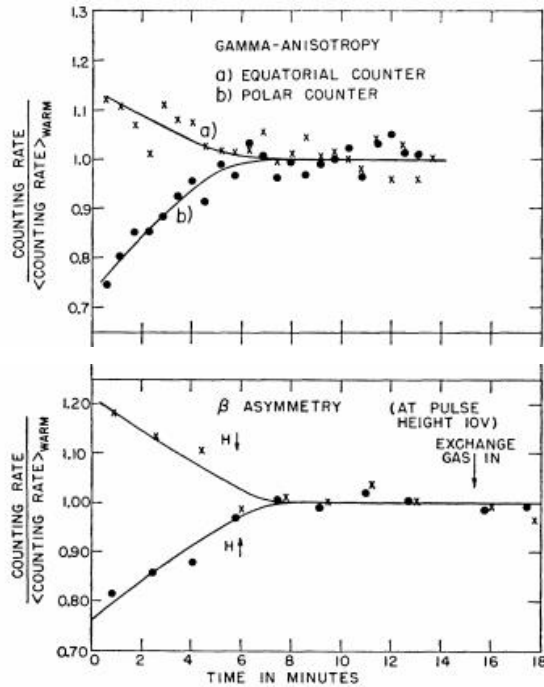


Figure 6: Gamma anisotropy and beta asymmetry for polarizing field pointing parallel and anti-parallel the β emission direction. The top plot of the gamma-anisotropy is count rate *vs.* time. The asymmetry in count rates from the detectors is γ -ray emission distribution from polarized nuclei which becomes random at approximately eight minutes. The lower plot is of the β -asymmetry in count rate *vs.* time. The asymmetry occurs under the reversal of the polarization of the ^{60}Co nuclei and disappears at approximately the same time as the γ anisotropy which is when the source loses polarization. Figure taken from Ref [15].

In addition, the beta asymmetry that was detected did not change signs with the reversal of the demagnetization field [15], which indicated that the asymmetry was not caused by permanent magnetization of the source.

The results of the experiment indicated the violation of parity in the weak interaction as more β particles were emitted of one helicity over the other.

1.4.4 The Violation of Parity

The Wu experiment was an indication of the violation of parity symmetry as the measurements made in the untransformed and the parity transformed frames, were different. Lee and Yang also proposed an experiment which involved pion decay reaction:

$$\pi^+ \rightarrow \mu^+ + \nu \quad \text{and} \quad (6)$$

$$\mu^+ \rightarrow e^+ + 2\nu. \quad (7)$$

The π^+ is a spin-less particle while the μ^+ and ν both possess a spin of $\frac{1}{2}$. Thus, when the π^+ decays, the spin of the ν and μ^+ will be anti-parallel each other. However, if parity is first assumed to be violated, then the μ^+ will be biased in its polarization and prefer one helicity. Thus, an asymmetry in the angular distribution of the μ^+ emission would be an indication of parity violation. The spin orientation of the μ^+ can be measured by the detection of e^+ emitted in the decay of the μ^+ as the e^+ will have the same spin as the μ^+ by conservation of angular momentum. If an asymmetry in number of e^+ of each helicity from the rest frame of the μ^+ were measured, then parity would be violated. The proposed experiment, showing indications of parity violation in the decay, was performed by Garwin et al. in 1957 [16] and published in the same issue of Physical Review as the Wu experiment. By 1957, the violation of parity had become well established and Lee and Yang won the Noble prize in physics in 1957 [1] for their prediction and proposal of the experiments.

1.5 Testing for Conservation of Parity

The third experiment suggested by Lee and Yang [2] provided the basis for the experiment outlined within this thesis. The experiment had, at first, been thought by Lee and Yang to be impossible to perform, as they did not believe that the circular polarization of γ -rays could be measured [2]. As is outlined by Schopper [19], were later discovered means to measure the circular polarization of γ -rays.

The circular polarization of γ -rays indicates which helicity an emitted γ -ray possesses. The experiment is similar to that of C.S. Wu et al. [2]. However, rather than polarizing the ^{60}Co and counting the number of β -particles emitted parallel and anti-parallel the nuclear spin of the ^{60}Co , γ -rays that are produced from the de-excitation of the daughter product of ^{60}Co , ^{60}Ni , are counted in coincidence with β -particles when the γ -rays leave the nucleus at 180° relative the β emission direction. By detecting γ -rays in coincidence with β -particles both emitted 180° each other's motion and collinear the nuclear spin of the ^{60}Co , from angular momentum conservation they will be circularly polarized and possess a particular handedness, while the emitted β -particles will possess opposite handedness. In the mirror, the handedness of the γ -rays and β -particles are reversed.

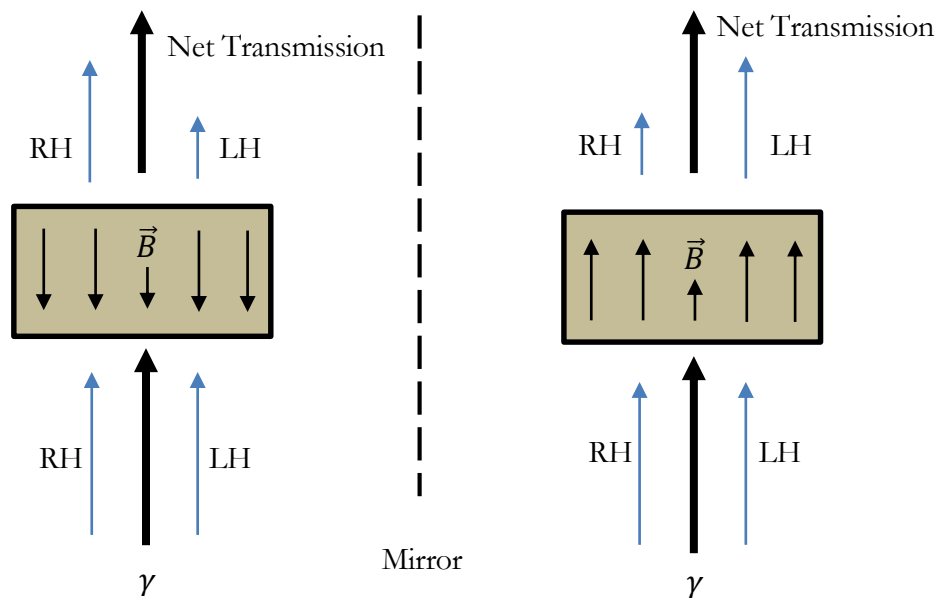


Figure 7: A diagram of the transmission of γ -rays through an electromagnet as occurs in this experiment. The length of the arrows labeled RH and LH indicate the relative number of right-handed γ -rays to left-handed γ -rays while the middle arrows below and above the magnet indicate the net number of incident and transmitted γ -rays, respectively. If parity is conserved, then there are expected to be equal number of left and right circularly polarized γ -rays incident the electromagnet. This will lead to a γ -ray transmission rate in equal number when the magnetic field is oriented parallel and anti-parallel the incident γ -rays. Note, however, that the direction of the magnetic field is not a product of the reflection transformation, but, rather, was used to distinguish between the left and right-handed coordinate systems as circularly polarized γ -rays will Compton scatter differently depending on the handedness of incident γ -rays and the direction of the magnetic field.

An electromagnet sets up a magnetic field and the electrons within the electromagnet become polarized in the direction of the magnetic field. The transmission of γ -rays through an electromagnet when the electrons within the electromagnet are polarized parallel and anti-parallel the incident circularly polarized γ -rays is different for left-handed and right-handed γ -rays. The probability of one handedness of γ -ray being transmitted through the electromagnet is dependent on the Compton Scattering cross section on polarized electrons. Thus, γ -rays of one handedness will be more likely to be transmitted through the electromagnet than the other handedness when the magnetic field is oriented so that particular handedness is more likely to exit the electromagnet than the other handedness. This can be seen in Figure 7 where parity symmetry is assumed conserved while in Figure 8 is assumed violated.

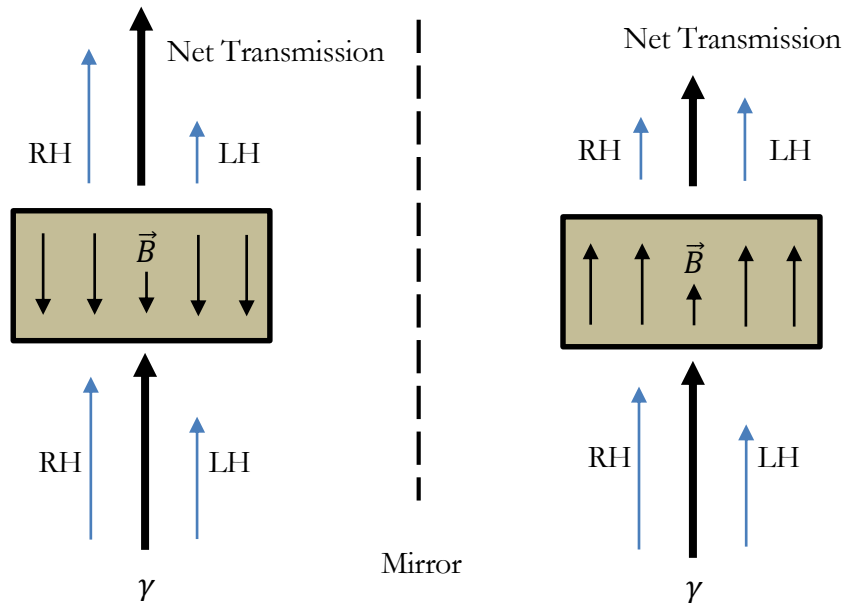


Figure 8: A diagram of the transmission of γ -rays through an electromagnet. The length of the arrows labeled RH and LH indicate the relative number of right-handed γ -rays to left-handed γ -rays while the middle arrows above and below the magnet indicate the net number of incident and transmitted γ -rays, respectively. If parity is violated, then there will be more γ -rays with one sense than the other incident the electromagnet. This will result in the more frequently emitted circular polarization increasing the net transmission rate for the orientation of the magnetic field that transmission through the electromagnet is more likely for that helicity. This results in a lower net transmission rate for the other helicity even when the magnet is oriented so that it is more likely to be transmitted as there are fewer γ -ray emissions from the ^{60}Ni of that helicity. Once again, the direction of the magnetic field is shown for reasons stated in Figure 7.

By measuring the transmission of γ -rays through the electromagnet, if no asymmetry in the count rate is observed by the reversal of the electromagnet polarity is observed, then there were the same number of left-handed and right-handed γ -rays in the de-excitation of ^{60}Ni . However, if an asymmetry is observed, then this indicates one handedness of γ -ray is emitted more frequently, a violation of parity symmetry. This is because a higher net transmission rate for one orientation of the magnetic field indicates that γ -rays of the helicity more likely to be transmitted were being more frequently emitted from their parent ^{60}Co nuclei shown on the left in Figure 8. Likewise, for the lower net transmission rate shown in Figure 8, the γ -rays with handedness more likely to be transmitted through the electromagnet are fewer in number, thus, the total γ -ray transmission through the electromagnet would be different for the two orientations of the magnetic field within the electromagnet.

2.1 Spin, Polarization, and Momentum Conservation

The experiment described in this thesis used the handedness of electrons and circularly polarized γ -rays emitted in the beta decay of ^{60}Co to make measurements of parity symmetry. The nature of beta decay in ^{60}Co will first be introduced.

The beta decay process of ^{60}Co is,



where the daughter product ^{60}Ni is in one of two excited states, as shown in Figure 9. The excited states of ^{60}Ni will further decay by γ emission, emitting one or two γ -rays depending on the angular momentum of the ^{60}Ni before it reaches the ground state. Therefore, every time an electron is emitted, at least one gamma ray is emitted simultaneously. As was previously stated, the β particles emitted will have an energy distribution due to sharing energy with the simultaneously emitted anti-neutrinos. For ^{60}Co , the β particle endpoint energy is 0.31 MeV for 99.88% of decays that occur and 1.48 MeV for the remaining 0.12%. After β emission, the excited ^{60}Ni nucleus will emit either a 1.1732 MeV and a 1.3325 MeV γ -ray or it will only emit the 1.3325 MeV γ -ray. The frequency with which the beta decay results in the emission of one γ -ray is very small in comparison to the frequency of emitting two. The case where two γ -rays are emitted can be ignored as they are all spin $J = 2$ γ -rays along the direction of nuclear spin. The γ -rays and electrons emitted when two γ -rays are emitted in ^{60}Ni reaching the ground state will be used in order to make measurements of γ -rays emitted 180° relative the electrons emission direction and, consequently, will be used to measure the violation of parity in the experiment outlined in this thesis.

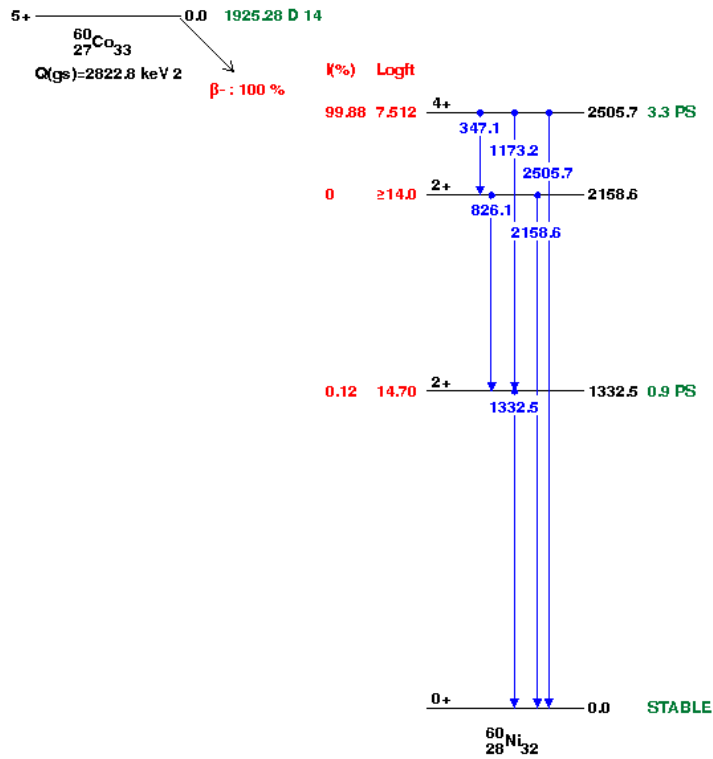


Figure 9: ^{60}Co Decay scheme. ^{60}Co nuclei possess a spin of 5+ and then decay by beta emission by emitting an electron and anti-neutrino to an excited state of ^{60}Ni . The ^{60}Ni will either be in the excited state with spin of 4+ and emit 1.1732 MeV and 1.3325 MeV γ -rays to de-excite or they will possess a spin of 2+ and decay by emitting a single 1.3325 MeV. The latter decay, however, is very unlikely, occurring only 0.12% of the time. For the purpose of the experiment outlined in this thesis, this excited state with a single emission of a γ -ray will be ignored. Figure taken from Ref [21].

In order to determine the handedness of the emitted particles in the beta decay of ^{60}Co , the nature of spin must first be discussed as the handedness of particles depends on their spin. The ^{60}Co decay products each possess intrinsic angular momentum. By conservation of angular momentum, if the orientation of the parent nucleus is known, then the spin of the daughter products may be determined.

As shown in Figure 10, when initially excited, the ^{60}Ni has a spin of 4. However, it then emits two circularly polarized γ -rays each with angular momentum 2 as indicated by the decay scheme in Figure 9 in order to conserve angular momentum. Adding the spins of each of the decay products of ^{60}Co including the spin of the γ -rays yields the spin of the ^{60}Co with a spin of 5. Because of this, the spin of the γ -rays will be in the same direction as that of the electrons emitted in the decay of ^{60}Co , and of the parent and daughter nuclei.

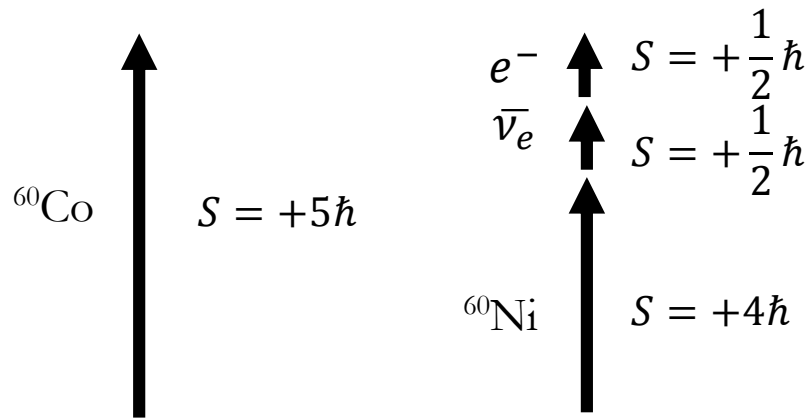


Figure 10: The diagram illustrates the parallel spins of the parent nucleus and the beta decay products. The arrows correspond to the spin of each particle. By conservation of angular momentum, the spins of the decay products sum to the spin of the parent nucleus.

This is imperative to the experiment as it guarantees that the spin of the γ -rays and electrons will be the same for every decay and that only the emission angle differs between the decays. However, as will be seen in the following section, the emission angle indicates what handedness the γ -rays and electrons have as they are emitted for a given spin orientation of ^{60}Co .

2.2 Helicity

The helicity of particles can be used to compare the mirrored interaction to the non-mirrored interaction. The helicity of a particle is defined as $h = \vec{J} \cdot \hat{p}$ where \vec{J} is total angular momentum and \hat{p} is the direction of the particle's momentum. Therefore, since total angular momentum is the sum of the orbital angular momentum, \vec{L} and the spin of the particle \vec{S} , then $h = \vec{L} \cdot \hat{p} + \vec{S} \cdot \hat{p}$. However, orbital angular momentum, by definition, is always orthogonal to the linear momentum as $\vec{L} = \vec{r} \times \vec{p}$. So, $\vec{L} \cdot \hat{p} = 0$ and, consequently, $h = \vec{S} \cdot \hat{p}$. For a particle traveling with some momentum in the \hat{p} direction with an intrinsic spin of \vec{S} , the particle is right or left-handed if the spin and momentum are parallel or anti-parallel, respectively. For example, for a spin- $\frac{1}{2}$ particle, like an electron, if the z-component of spin has eigenvalues of $\frac{\hbar}{2}$ and $-\frac{\hbar}{2}$, then when the momentum is in the z-direction, the helicity is either $h = \frac{\hbar}{2}$ or $h = -\frac{\hbar}{2}$ corresponding to right-handed and left-handed beta particles, respectively. Under a reflection transformation, the helicity of a particle will reverse. This is because, as illustrated in Figure 1, the direction of the angular momentum is reversed in the mirror though the particle's direction is not reversed in the mirror if traveling along the z-axis. Hence, the projection of the particle's momentum onto the z-axis will differ between particles moving parallel and anti-parallel the nuclear spin by a negative sign. Because the helicity indicates what handedness the particle is, a preference in the helicity of transmitted γ -rays indicates a preference in handedness.

An important property of the neutrino in beta decay is its helicity. The helicity of a neutrino (or anti-neutrino) is always the same in all reference frames. The reason is that it is a nearly massless particle and, thus, travels at approximately speed of light. Consider a particle that has mass moving with a momentum \vec{P} with a spin of \vec{S} . Then, from a reference frame that was not moving, point \mathcal{P} in Figure 8, the particle would appear to be right-handed; that is, its angular momentum and its momentum would be parallel. If point \mathcal{P}' was moving away from the particle faster than \vec{v} , then the particle would be left-handed according to an observer at point \mathcal{P} . Because of this, the helicity of the particle will have reversed, as a

result of the relative motion of the observer, as the direction of velocity and spin which, at first, were parallel, are now anti-parallel, changing the particle's helicity.

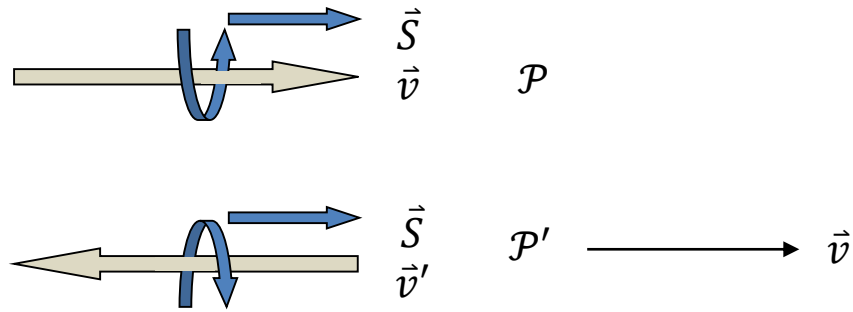


Figure 11: The vectors on the top left represent the helicity of a particle when an observation point \mathcal{P} is motionless. The lower left vectors represent the helicity of the particle when the point \mathcal{P} is accelerating away from the particle, thus, reversing the helicity observed at \mathcal{P} .

Because neutrinos are near mass-less and therefore travel at approximately the speed of light, all observers will agree on the helicity of the neutrino. Only left-handed neutrinos and right-handed anti-neutrinos [14] have ever been detected due to maximal parity violation in the weak interaction.

2.3 Indicator of Parity Violation

The conservation of angular momentum can be utilized to compare right-handed and left-handed γ -rays in coincidence with electrons of the opposite helicities emitted in the opposite direction. For a ^{60}Co nucleus with nuclear spin oriented in the $+z$ direction, as shown in Figure 12, the emitted γ -rays and electrons will both possess spin along the $+z$, as well, to conserve angular momentum. Because the emission angle determines the helicity of the particle, then, in the simple case outlined in Figure 12 where the emission direction of the γ -ray and electron are collinear the nuclear spin of the ^{60}Co , then the γ -rays are circularly polarized and are right-handed, while the electron is left-handed. Their helicities are reversed when observed in the mirror as the direction of spin is reversed under the reflection transformation yet the emission directions of the γ -ray and electron under consideration in Figure 12 are left unchanged. Under the reflection transformation, the decay on the right in Figure 12 is the mirror

of the decay on the left in Figure 12. Consequently, the decay on the right in Figure 12 becomes a left-handed coordinate system allowing for the measurement between the decay in a right-handed and left-handed coordinate system which is necessary to test for the violation of parity symmetry.

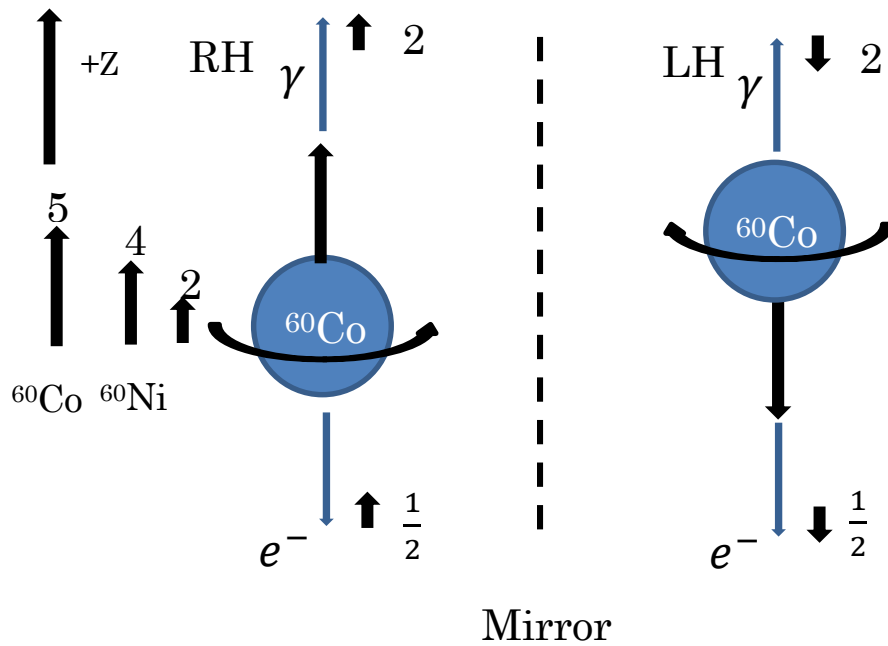


Figure 12: A ^{60}Co nucleus with spin oriented in the $+z$ direction. ^{60}Co , with a spin of 5, will decay into ^{60}Ni with spin of 4 and the ^{60}Ni will decay by emitting two γ -rays with spin 2. Though γ -rays and electrons will follow a distribution for emission, the decay shown, if only one γ -ray is considered (the one emitted opposite the electron's momentum), results in γ -rays that are circularly polarized.

Though the emission of gamma rays from the ^{60}Co will follow an angular distribution, however, the projection of the momentum of the gamma rays onto the $+z$ axis in Figure 8 will be positive for right-handed gamma rays and negative for left-handed. Consider the simplified case where only the γ -rays emitted in the $z+$ direction opposite the electrons are considered as shown in Figure 12. In this configuration, the γ -rays are both collinear the spin of the ^{60}Co nucleus and are, thus, circularly polarized.

If measurements made of the decay and the mirror presented in Figure 12 are both measured with the same frequency, then parity is conserved. However, if measurements of the number of right circularly polarized γ -rays differ the number of left circularly polarized γ -rays (the mirror in Figure 12) when counted in coincidence with the electrons emitted opposite the γ -rays, then this is an indication of parity violation as there exists a preference in helicity making the decay distinguishable from the mirror. If the number of right circularly polarized and left circularly polarized γ -rays detected in coincidence with the opposite emitted electrons are measured in equal frequency, then the decay and the mirror are indistinguishable and parity symmetry is conserved.

2.4 Calculations of Count Rate Estimates

2.4.1 Measurement of Circular Polarization of Gamma Rays

As outlined by Schopper [19], the polarization of circularly polarized gamma rays emitted during the decay of nuclei via beta decay be experimentally measured. Schopper concluded that a feasible method for determining the circular polarization of gamma rays is transmission through a magnet. Compton scattering of circularly polarized γ -rays from polarized depends on the orientation.

The differential Compton scattering cross section for circularly polarized γ -rays by polarized electrons [19] is

$$d\sigma = \frac{r_0^2}{2} \left(\frac{k}{k_0} \right)^2 \{ \phi_0 + P_1 \phi_1 + f P_c \phi_c \} \quad (9)$$

where r_0 is the classical electron radius, \mathbf{k}_0 is the initial photon momentum, \mathbf{k} is the photon momentum after scattering, P_1 is the degree of linear polarization and is positive if the electric vector \mathbf{E} is perpendicular to the $(\mathbf{k}_0 \mathbf{k})$ -plane, negative if \mathbf{E} lies in the plane of scattering, P_c is the degree of circular polarization of the photons and is positive if the radiation is right circularly polarized, and f is the fraction of oriented electrons. The ϕ_0 function gives the ordinary Compton cross sections first derived by Klein-Nishina [20], and ϕ_1 and ϕ_c are the polarization dependent parts of the cross section:

$$\phi_0 = 1 + \cos^2 \theta + (k_0 - k)(1 - \cos \theta) \quad (10)$$

$$\phi_1 = \sin^2 \theta \quad (11)$$

$$\phi_c = -(1 - \cos \theta)[(k_0 + k)\cos \theta \cos \psi + k \sin \theta \sin \psi \cos \varphi] \quad (12)$$

where θ is the scattering angle, ψ is the angle between the direction of the incident photon \mathbf{k}_0 and the electron spin \mathbf{S} and φ is the angle between the $(\mathbf{k} \mathbf{S})$ -plane and the $(\mathbf{k}_0 \mathbf{k})$ -plane as is seen in Figure 13.

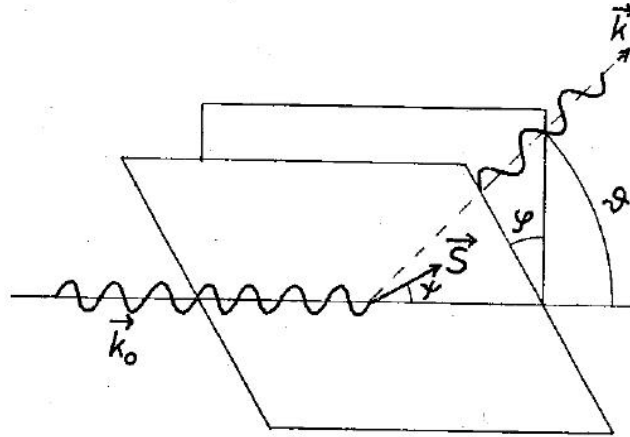


Figure 13: Compton scattering from polarized electrons. \mathbf{k}_0, \mathbf{k} momentum incident of scattered photon, respectively, \mathbf{S} electron spin. Figure taken from Ref [19].

By using the differential scattering cross section, the polarity of incoming circularly polarized gamma rays can be determined as they will have some probability of Compton scattering as they travel through an electromagnet. The Compton cross section is proportional to the probability that Compton scattering

of the γ -rays on polarized electrons within the magnet will occur. The cross section for Compton scattering when the spin of the polarized electrons within the magnet and the incident gamma rays are parallel is different from when they are anti-parallel. The electrons within the electromagnet's iron core can be polarized parallel and anti-parallel the circular polarization of the gamma rays. Since the polarization of the magnet can be known directly when the magnet is polarized, the polarization of the gamma rays can also be determined from this which indicates their handedness.

2.4.2 Cross-section Calculations

In order to determine the direction of circular polarization of the photons, gamma rays transmitted through the magnet may Compton scatter on electrons polarized parallel and anti-parallel the incident photons. Since the cross section for Compton scattering as seen in Equation 9 is different for photons with spin parallel and anti-parallel the polarized electrons within the magnet, the circular polarization of the gamma rays can be determined by measuring the asymmetry in fraction transmitted. The total cross-section for Compton scattering is obtained from integrating the differential Compton scattering cross-section in Equation 9 over θ and ϕ which gives,

$$\sigma = \sigma_0 + fP_c\sigma_c \quad (13)$$

where

$$\sigma_c^\pm = \pm 2\pi r_0^2 \left(\frac{1 + 4k_0 + 5k_0^2}{k_0(1 + 2k_0)^2} - \frac{1 + k_0}{2k_0^2} \ln(1 + 2k_0) \right) \quad (14)$$

with the positive and negative σ_c corresponding to electron spin parallel and antiparallel the photon spin, respectively, giving the total cross section for Compton scattering a polarization dependency, which is required to distinguish between right circularly polarized and left circularly polarized γ -rays.

2.4.3 Correlation between Circularly Polarized γ -Rays and β Particles

To estimate the count rate of γ -rays transmitted through the electromagnet, let N_0 be the number of gamma rays incident on the magnet, as shown in Figure 14. Then, inside the magnet at a distance, x , the number of gamma rays that are scattered out of the beam after traveling a distance $x + \delta x$ is

$$N_s = N(x) - N(x + \delta x). \quad (15)$$

where N_s is the number of scattered γ -rays. However, the number of scattered gamma rays is known from the cross section, hence,

$$N_s = \sigma N'_t N_{inc} \delta x \quad (16)$$

where N'_t is the number of electrons on which the γ -ray can Compton scatter.

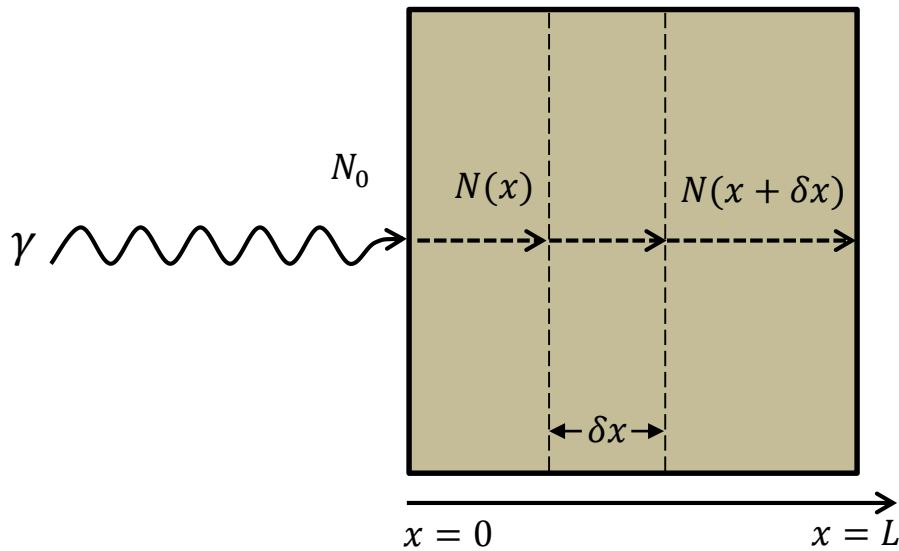


Figure 14: Attenuation of γ -rays by magnet core of length L . If there are initially N_0 γ -rays incident the magnet, then consider a depth x within the core. There will be $N(x)$ γ -rays. The number of γ -rays initially at a distance x that do not Compton scatter, but move a distance δx into the magnet is $N(x + \delta x)$. The number of γ -rays that scatter are the number of γ -rays at $N(x)$ minus the number of γ -rays after reaching a distance $N(x + \delta x)$ through the magnet.

Therefore, we have,

$$N(x) - N(x + \delta x) = \sigma Z N_t N(x) \delta x . \quad (17)$$

where Z is the number of electrons per atom, N_t is the iron atom number density, and σ is the cross section for Compton scattering. So, in the limit as $\delta x \rightarrow 0$,

$$\frac{dN}{dx} = -\sigma Z N_t N(x) . \quad (18)$$

Therefore, upon integrating,

$$N(x) = N_0 e^{-\sigma Z N_t x} . \quad (19)$$

From the total cross section in Equation 13, we have two count rates as the differential cross section is dependent on whether the electron spins within the iron are parallel or anti-parallel the photon spin. Thus, by Equation 13, we have that,

$$N_+ = N_0 (e^{-\sigma_0 Z N_t x} e^{-f P_c \sigma_c Z N_t x}) . \quad (20)$$

$$N_- = N_0 (e^{-\sigma Z N_t x} e^{f P_c \sigma_c Z N_t x}) . \quad (21)$$

where N_+ and N_- are the count rate of gamma rays after passing through a material of thickness x for electron spins within the iron that are parallel and anti-parallel the photon spins, respectively. Therefore, the asymmetry in count rate when the magnetic field, and hence the electron spin direction is reversed is,

$$E = \frac{N_+ - N_-}{\frac{1}{2}(N_+ + N_-)} . \quad (22)$$

After substituting for N_+ and N_- ,

$$E = 2 \tanh(-fP_c\sigma_cZN_t x) = 2 \tanh(-N_t\nu\sigma_cP_c x) . \quad (23)$$

where $\nu \equiv Zf$, the number of oriented electrons per iron atom, yielding an asymmetry in agreement with Schopper [19].

Using Equations [22] and [23], which are estimates for the asymmetry in the count rates, plots of the estimates for the asymmetry were made as functions of thickness of the electromagnet, then as a function of the initial energy of the γ -rays and then as a function of the collection time of γ -ray transmission for each orientation of the magnetic field on the electromagnet. The asymmetry as a function of thickness can be seen in Figure 15 with a fixed initial energy of 1.33 MeV and a fixed initial collection time of ten days.

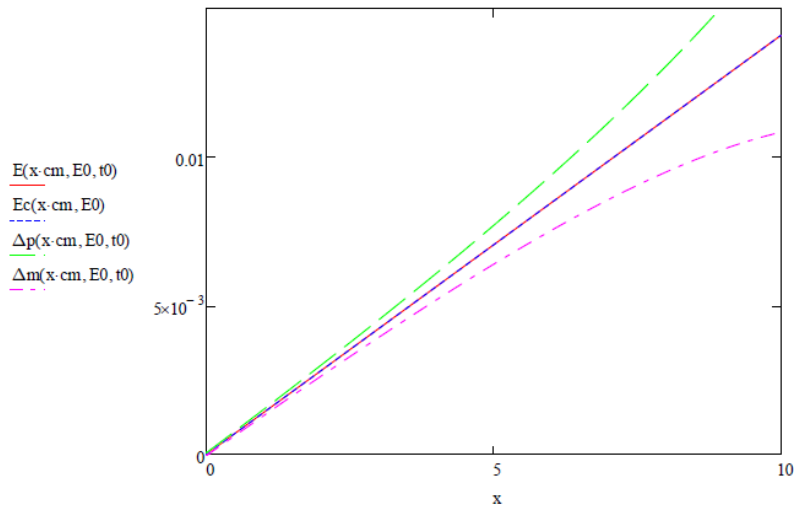


Figure 15: The asymmetry in count rate with the uncertainty as a function of magnet thickness. The thickness x is in units of cm. The dashes represent the uncertainty in the asymmetry. The collection time and initial incident γ -ray energy are fixed at 10 days and 1.33 MeV, respectively. Both the Equation 22 and 23 for the count rate are plotted and lie directly on top of each other.

The asymmetry as a function of initial γ -ray energy is shown in Figure 16 with a fixed thickness of 9.3 cm, the thickness of the electromagnet used in this experiment, and a fixed collection time of ten days.

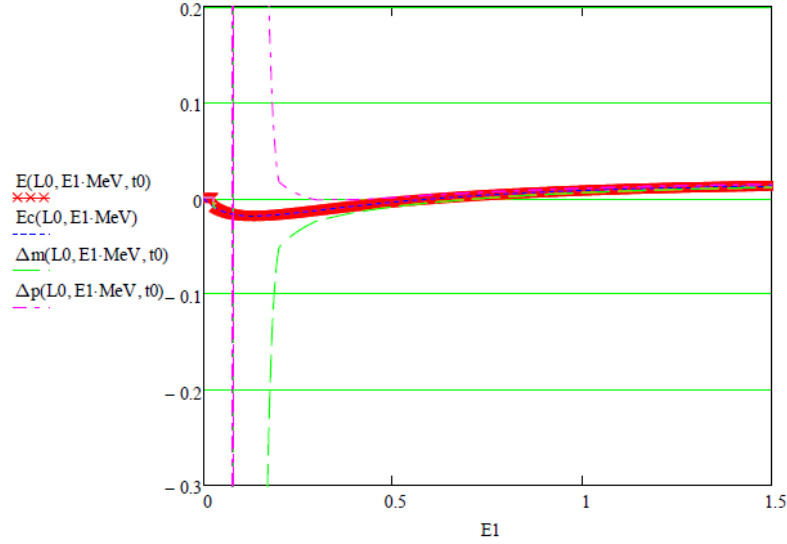


Figure 16: Asymmetry and the uncertainty both as a function of the initial energy of the incident γ -rays in MeV. The collection time and the thickness of the magnet are fixed at 10 days and 8 cm, respectively. The dashes represent the uncertainty in the asymmetry of the count rate. Both the Equation 22 and 23 for the asymmetry are plotted and lie directly on top of each other.

The asymmetry as a function of collection time can be seen in Figure 17 with a fixed thickness of 9.3 cm, and a fixed initial γ -ray energy of 1.33 MeV.

For this experiment, a relative uncertainty in the asymmetry of approximately 5% is intended to be achieved, if possible. The approximate relative uncertainty was determined to be as follows:

$$\Delta E = \frac{1}{\sqrt{2N_0}} \left(\frac{e^{-N_t \nu \sigma_c x}}{\nu N_t \sigma P x} \right). \quad (24)$$

Figure 18 shows the relative asymmetry as a function of the collection time. The calculation shows that, in order to achieve a relative uncertainty of approximately 5% requires a collection time of approximately two days. Thus, to make measurements of the γ -ray transmission through the electromagnet for both polarities of the electromagnet have been estimated to take approximately 100 days total. This can be reduced greatly by decreasing the thickness of the electromagnet as the uncertainty in the asymmetry, as shown in Figure 15, is strongly affected by the thickness of the electromagnet.

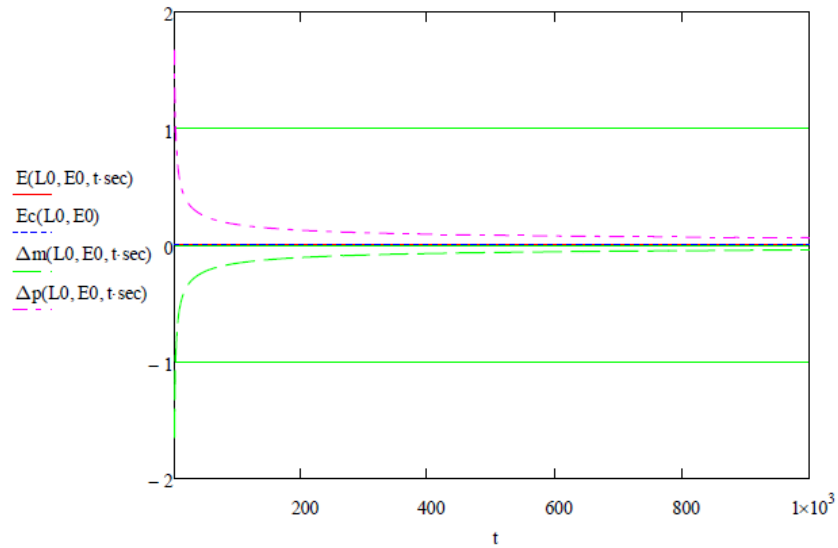


Figure 17: Asymmetry and the uncertainty both as a function of the collection time. The units of time t is seconds. The dashes represent the uncertainty in the asymmetry. The thickness of the magnet and the initial incident γ -ray energy are both fixed at 8 cm and 1.33 MeV, respectively. Both the Equation 22 and 23 for the count rate are plotted and lie directly on top of each other.

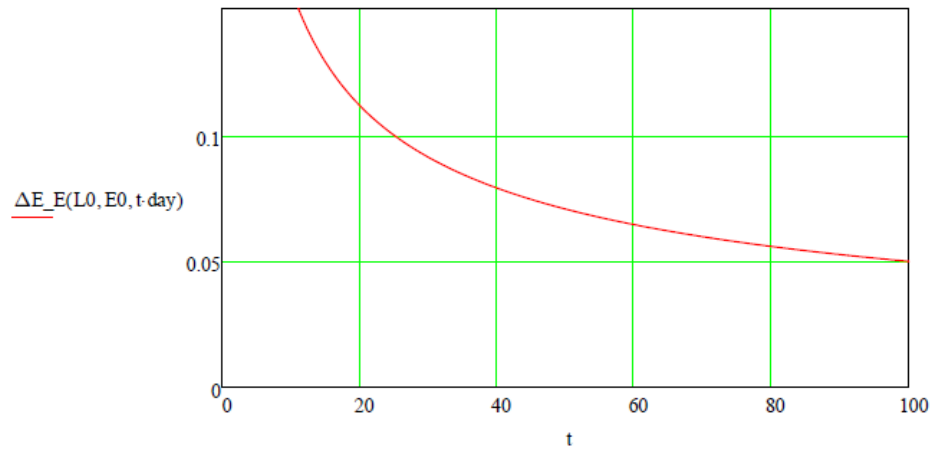


Figure 18: Relative uncertainty as a function of collection time where time is in days. The thickness of the magnet and the initial incident γ -ray energy are both fixed at 8 cm and 1.33 MeV, respectively.

3.1 Description of Apparatus

As described in Section 1.5.1, the asymmetry in the transmission of circularly polarized γ -rays through an electromagnet can be used to probe for parity violation. Electrons that are emitted from ^{60}Co opposite to γ -rays incident the electromagnet will be measured in coincidence with the γ -rays to ensure that the γ -rays are circularly polarized, as required by angular momentum conservation shown in Figure 12. Though the γ -rays and electrons emitted will follow a distribution, by using coincidence measurements of the γ -rays and electrons emitted 180° with respect to each other it can be ensured that for γ -rays of one helicity, an electron of the opposite helicity will be measured and that the γ -rays will be circularly polarized, following the decay configuration as shown in Figure 12.

The apparatus used to perform coincidence measurements consisted of a Nuclear Instruments Module (NIM) circuit, an electromagnet for determining the polarization of gamma rays, a Germanium detector for γ -rays and a Silicon surface barrier detector electrons, and a ^{60}Co source as can be seen in Figure 19.

The approximately $1\ \mu\text{Ci}$ ^{60}Co source emits beta particles which were detected by a Amtek BA-014-025-1000 Silicon surface barrier detector that is 1.78 cm in diameter and 1.27 cm thick. The signal was then sent to the NIM circuit, a fast-timing coincidence circuit that recorded the energy spectrum of transmitted γ -rays in coincidence with the emitted electrons. Before detection, the γ -ray traversed the core of a 46W Magnetech R-60 30-24 electromagnet with a diameter of 7.62 cm and a thickness of 6.35 cm, collinear and opposite the beta particle's path. The gamma rays that left the electromagnet within the solid angle of the Tennelec ERVDS30-16215 High Purity Ge detector with a diameter of 7.62 cm and a length of 23.37 cm were detected. The signal was then integrated by the pre-amplifier attached to the Ge detector and was sent to the NIM circuit for signal shaping and processing.

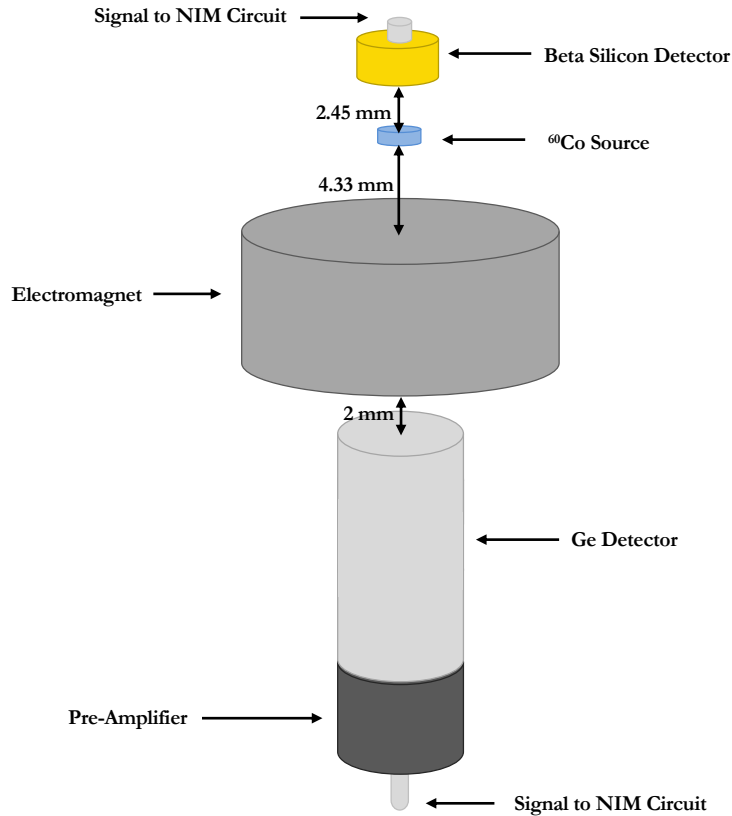


Figure 19: A diagram of the apparatus used in experiment. A silicon detector and a Ge detector were used to detect beta particles and gamma rays, respectively. The outputs from the detectors were sent to a fast-timing NIM coincidence circuit. For the γ -rays from the ^{60}Co , only the γ -rays that are transmitted through the electromagnet will be detected in the Ge detector.

A Ge detector was used as it offered a higher energy resolution which is important to reduce signal noise due to accidental coincidence. The Ge detector was attached to a cylindrical Tennelec LN₂ Dewar with a volume of approximately $14.1 \times 10^3 \text{ cm}^3$ in order to cool the Ge detector. The Ge detector was also surrounded by stacked 13.5 mm deep lead rings in order to shield it from background radiation. The Dewar and lead shielding can be seen in Figure 20. Initial measurements were made to determine

whether additional shielding was required. Energy spectra of γ -rays from the ^{60}Co used in the experiment showed that the lead shielding was sufficient as shown in Figure 28 by the low noise floor.

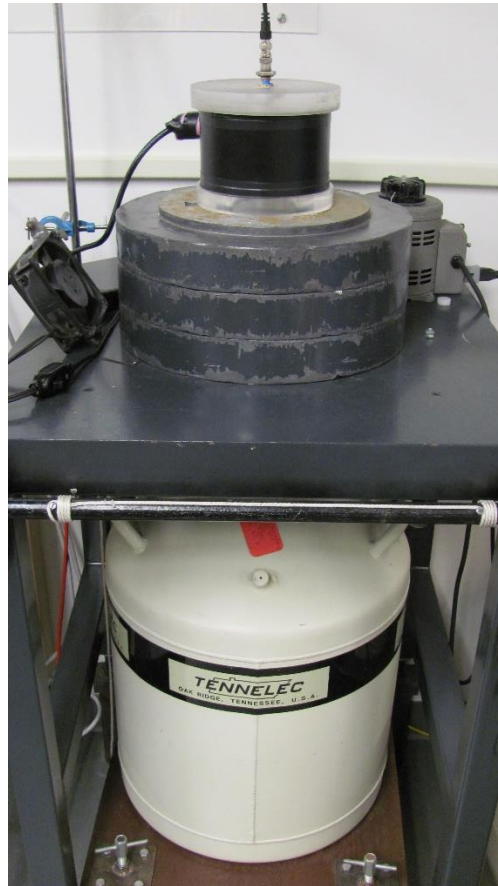


Figure 20: Photograph of the apparatus used in experiment. The electromagnet is placed between two pieces of acrylic. The top acrylic mount houses the ^{60}Co source used in the experiment and the bottom rests in a small cylindrically symmetric. The acrylic mounts assure the collinearity of the axes of the Silicon surface barrier detector, the source, the magnet, and the Ge detector. The radial thickness of the rings is 13.5 mm.

Two acrylic mounts were made to be placed atop and below the electromagnet to assume the collinearity of the detectors. The lower mount, which can be seen in Figure 21, was made for the electromagnet to

rest on. The lower mount surrounded the Ge detector to ensure that the central axis of the detector was aligned with the electromagnet.

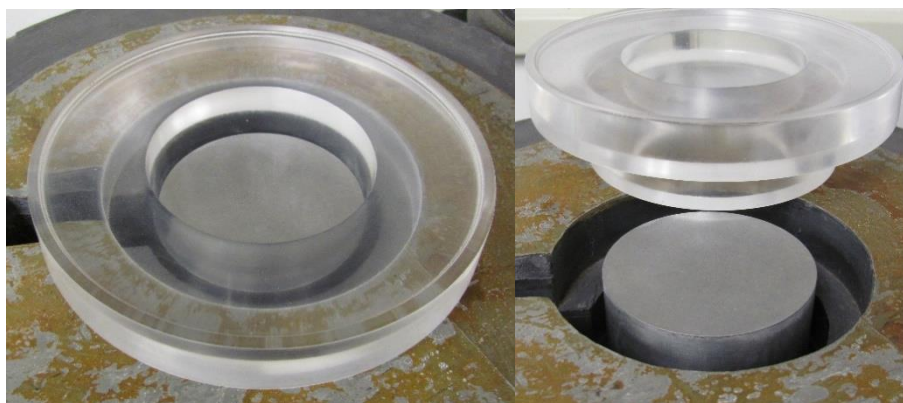


Figure 21: An acrylic mount that the electromagnet rested on. On the right, on the bottom of the mount can be seen a small lip. This rested between the top lead ring and the Ge detector so that the bottom acrylic mount did slide on the surface of the lead ring.

A second acrylic mount, the top mount shown in Figure 22, was placed on top of the electromagnet. A small cylindrical cavity was cut in the center to house the beta detector in order to align the central axis of the detector with the electromagnet and source. Furthermore, the ^{60}Co source that was used in the experiment was placed within the mount. A small removable acrylic ring was cut from the mount, shown in Figure 22 on the right. With the ring removed, a piece of $8.0264\ \mu\text{m}$ 1000 series aluminum foil was placed inside the, now larger cylindrical cavity, the source placed atop the foil, and the ring placed on top of the foil, with the foil also surrounding the sides of the acrylic ring.

A second cylindrical cavity was also made within the top acrylic plate. As seen in Figure 23, a cylindrical cavity at a depth of 4.07 mm below the cavity for the removable acrylic ring, shown in Figure 22, was made with the radius of the ^{60}Co source used. The aluminum foil lined the inside of this smaller cavity, as well.

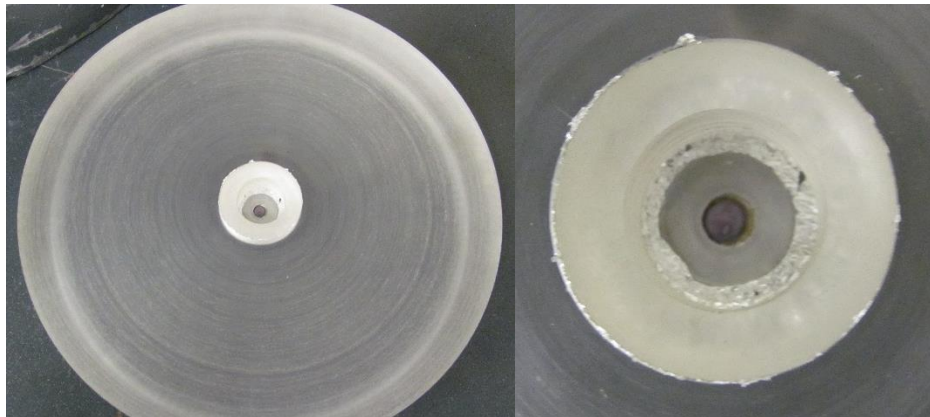


Figure 22: (left) A photograph of the acrylic mount described in Figure 20 was made to place on the top of the magnet. A thin piece of $8.0264\ \mu\text{m}$ 1000 series aluminum foil was placed inside a cutout made within the acrylic top mount. The ^{60}Co source shown in Figure 24 was placed inside the foil and a small acrylic ring with depth of 10.93 mm was placed within the cutout over the foil with the foil surrounding the ring placed within the cutout. The foil was used to ensure that the β -silicon detector which was placed within the cutout just above the ^{60}Co source, shown on the right, was light-tight.

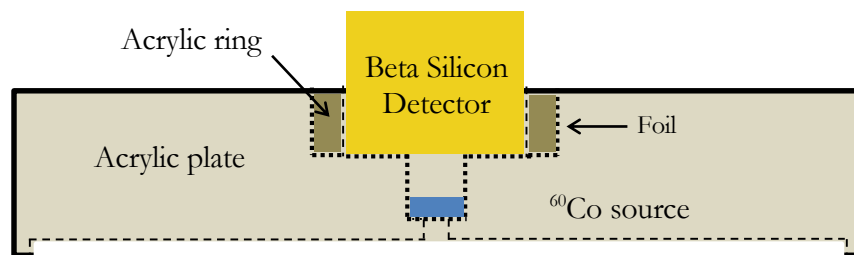


Figure 23: Cross section of the acrylic mount placed on top of the electromagnet. In order to increase the collinearity of the apparatus, the acrylic mount had two cuts of separate radii and each to different depths. The deepest was for the ^{60}Co source shown in the bottom cutout. Above this is the second cutout made for the beta silicon detector. Thin foil was placed inside both cutouts to the bottom of the cutout for the ^{60}Co source, as shown in Figure 22 and the ^{60}Co source was placed above this foil. The foil wrapped along the walls of the cutout and also surrounded the beta silicon detector, as well, in order to ensure that the detector was light-tight. An additional cylindrical cutout on the bottom of the mount was made, the diameter of the magnet, at a depth of 3.34mm to cap the magnet in order to keep the mount from sliding on the magnet.

polyethylene were hole-punched into identical disks of thickness 0.81 mm and diameter 12.96 mm. The electroplated ^{60}Co was placed between the two disks with the ^{60}Co source on the plate showing through the center of one of the disks as shown in Figure 24.

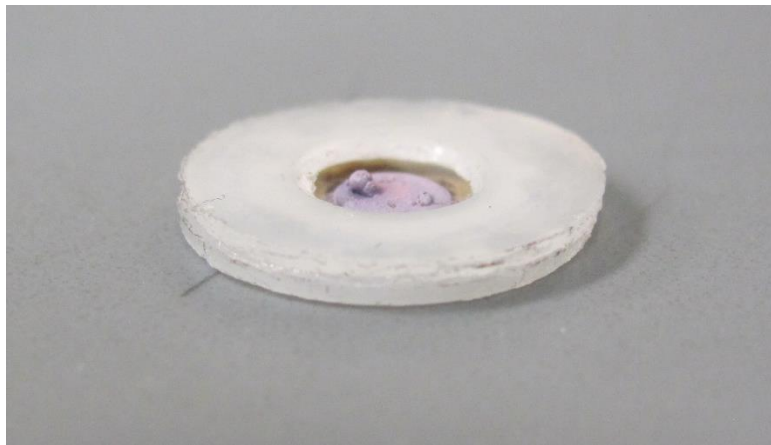


Figure 24: Radioactive source used in experiment. Approximately $1\ \mu\text{C}$ of ^{60}Co was electroplated to a thin piece of steel foil approximately 0.0508 mm thick which was cut into a circular disk shape. Two thin rings of polyethylene of thickness 0.81mm and with diameter of central cutout of 5.35mm were made. The thin foil with the ^{60}Co was placed in-between the two rings, exposing the ^{60}Co in the central cutout and the two rings were glued to the thin foil. This was placed within the piece of acrylic shown in Figure 22.

An image of the full apparatus used in the experiment, including the NIM circuit, is shown in Figure 25. The electromagnet was powered by a Hantek PPS2320A power supply that was kept at a current of 1.74A to prevent overheating of the magnet. The transmitted γ -ray energy spectrum in coincidence with the emitted electrons circuit was recorded on the laptop shown in Figure 25 for each polarity of the magnet current.

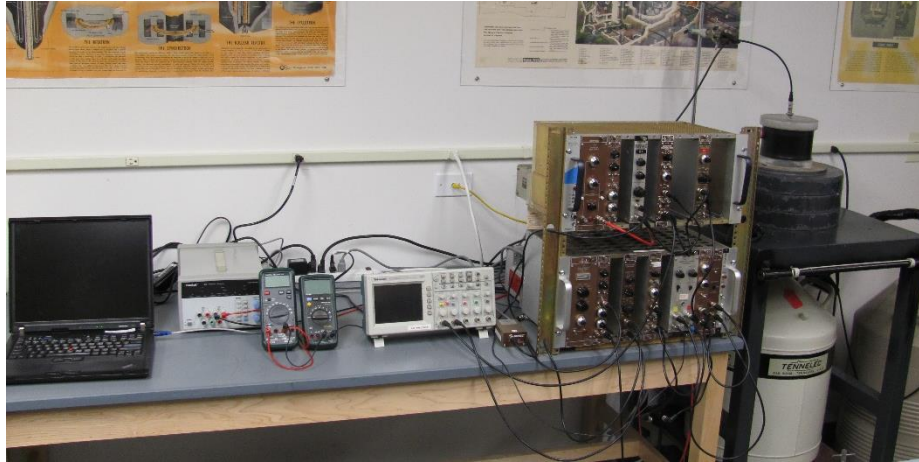


Figure 25: Photograph of the apparatus used in experiment. Included in the image is the detectors, the NIM circuit for shaping the signal received and forming coincidence, an oscilloscope to monitor the output signals from each module, a power supply for the electromagnet used in the experiment, and a laptop to record the timing and energy spectra.

A second measurement will be made when the current sent through the electromagnet is reversed by manually reversing the output leads on the power supply. This will yield two energy spectra. The count rates of the transmitted γ -rays can be used to test for an asymmetry in the γ -ray transmission as described in section 1.5.1. The process by which the NIM circuit, shown in Figure 25, shapes the signals output from both detectors will be described in the following section.

The electromagnet has a thickness of 61.33 mm. Steel plates of various thicknesses were placed on top of the electromagnet with a 12.7 mm gap in between and a gauss meter probe was placed in the gap reaching the center of the electromagnet. Measurements of the saturation of the electromagnet were made using each steel plate thickness, as well as with no plate, to determine what voltage the electromagnet should operate at.

The electromagnet began saturating at approximately 18-V with the 6.223 mm steel plate on the top of the magnet as is shown in Figure 27.

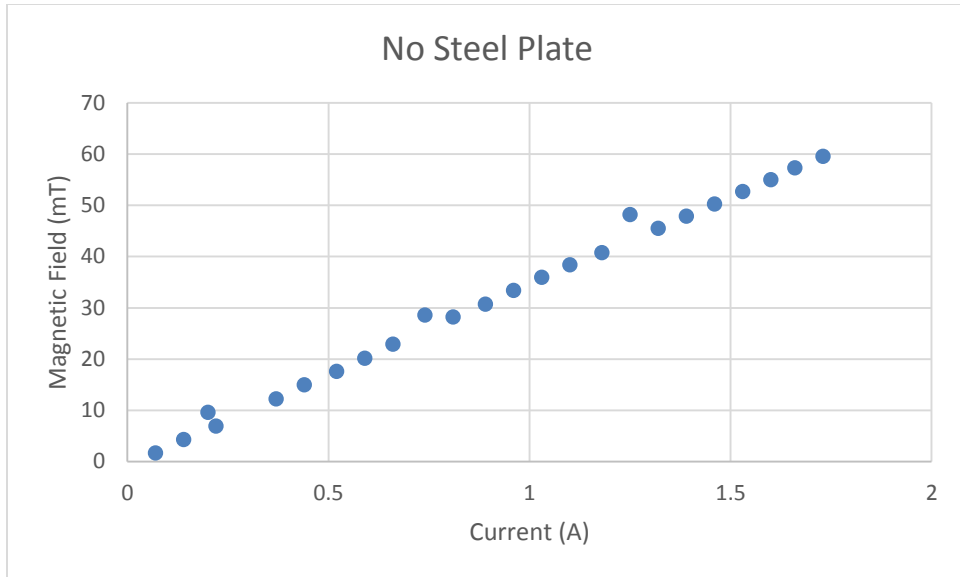


Figure 26: The magnetic field versus the current when no steel plate was placed on top of the electromagnet. No saturation of the magnet was seen between 2-V and 23-V operating voltage.

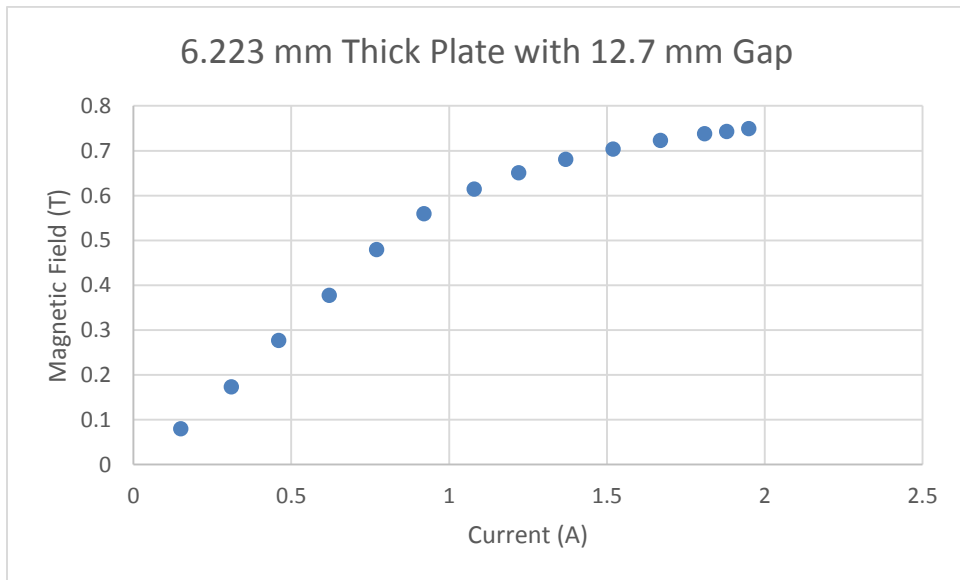


Figure 27: The magnetic field versus the current when a 6.223 mm thick steel plate was placed on top of the electromagnet with a 12.7 mm gap in between. Saturation of the electromagnet began at roughly 18-V operating voltage which was roughly a current of 1.37 A.

An axially symmetric cylindrical hole was made with diameter 25.38 mm through the length of the magnet and an iron rod of the same size as the cylindrical hole was placed within the electromagnet. The 6.223 mm steel plate was placed on top of the electromagnet with the 12.7 mm gap in between and a 10 mm steel plate was placed on the bottom of the electromagnet capping the iron rod within the electromagnet. Prior to the cut, measurements of the saturation of the electromagnet using the 10 mm steel plate on top using the same method described before to ensure that the electromagnet would still saturate with the thicker steel plate.

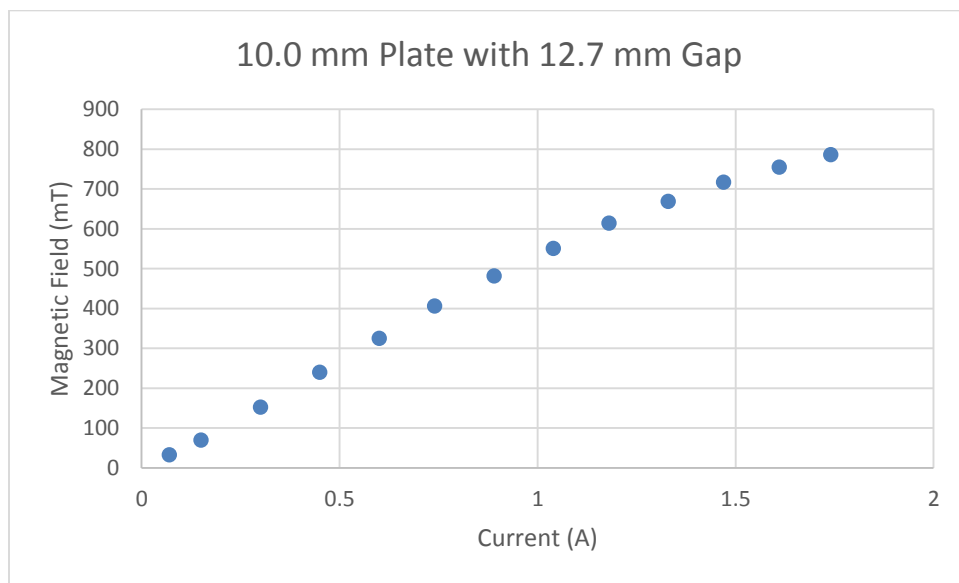


Figure 28: The magnetic field versus the current when a 10.0 mm thick steel plate was placed on top of the electromagnet with a 12.7 mm gap in between. Saturation of the electromagnet began at roughly 22-V operating voltage which was roughly a current of 1.61 A.

The electromagnet began saturating at roughly 22-V operating voltage at a current of approximately 1.61 A. Higher operating voltages than 24-V increased the temperature of the electromagnet to unsafe levels without cooling equipment and was kept at roughly 22-V for this reason.

3.2 Electronics

Coincidence γ - β measurements were performed with the fast-timing NIM coincidence circuit shown in Figure 29. Two signals were processed in the circuit in order to obtain coincidence measurements. The signal from the silicon beta detector was integrated by a pre-amplifier. The circuit then split the signal to both a spectroscopy amplifier and a timing filter amplifier.

The spectroscopy amplifier generated a Gaussian shape pulse with height proportional to the energy. A Amptek 8000A Pocket Multi-Channel Analyzer (MCA), then recorded the energy spectrum deposited in the silicon detector to ensure that the silicon detector was functioning properly and that the Constant Fraction Discriminator (CFD) threshold was set properly.

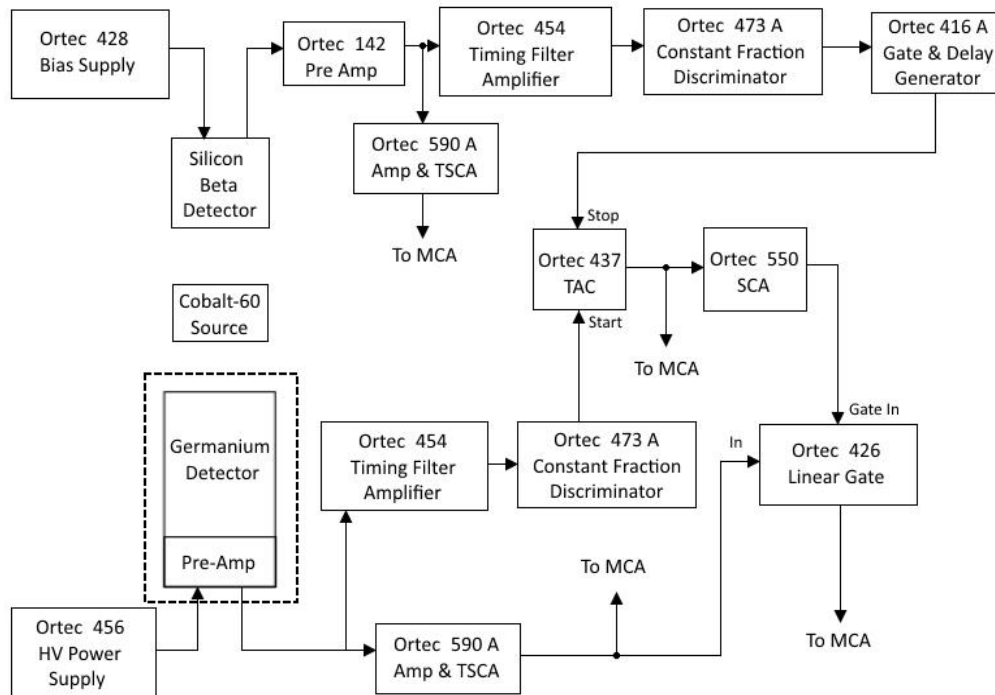


Figure 29: Fast-timing NIM Circuit. The NIM circuit processes signals coming from the Silicon Beta and Ge detector. The energy spectra of the electrons and γ -rays are obtained from the pocket Multi-Channel Analyzer and are sent to a laptop to be recorded in Amptek PMCA. Timing spectra are also obtained from the output of the Time-to-Amplitude Converter. The γ -ray transmission energy spectrum in coincidence with the detected electrons can also be recorded from the output of the Linear Gate to the Multi-Channel Analyzer.

The signal going to the Timing Filter Amplifier was differentiated, roughly shaping the signal back to what it was coming out of the silicon beta detector, making it a very fast pulse suitable for timing. A Constant Fraction Discriminator generated logic pulses from input signals exceeding a threshold. The differentiation of the signal by the Timing Filter Amplifier was necessary as the CFD requires a signal of roughly the shape of the direct output of a Photomultiplier Tube. The logic pulse was sent to a nanosecond delay to shift the zero-point of a Time-to-Amplitude Converter (TAC) to the middle of the timing spectrum to avoid cutting off half of the peak and then to the stop on the (TAC).

The signal from the Ge detector was integrated by the pre-amplifier attached to the Ge detector. The signal, then, was also split and input into a spectroscopy amplifier and to a Timing Filter Amplifier. The signal from the Timing Filter Amplifier entered a CFD which produced the logic pulse used to start the TAC. The TAC generated a unipolar Gaussian pulse with height proportional to the time difference between the start signal from the Ge detector and the stop signal from the silicon beta detector. The TAC output pulses were histogrammed by the MCA to obtain the timing spectrum. The timing spectrum was used to determine the timing resolution of the circuit. The SCA generated logic pulses when the input signal is within a set upper and lower discrimination voltage window. Thus, the SCA only generated logic pulses for time differences between the Ge and silicon beta detector signals that were small enough to be due to the same event, or “in coincidence.” The logic pulse from the SCA was then used to open a Linear Gate as Gate In signal, allowing signals from the Ge spectroscopy amp to enter the MCA. The window on the SCA was set wide enough to include the 1.17 MeV and 1.33 MeV energy γ -rays. The MCA created a histogram of the energy spectrum of the gamma rays that are in coincidence with the beta particles. The amplifier for the Ge detector signal was also used with an MCA to histogram the gamma ray energy spectrum for all gamma rays. This allowed for comparison of the energy spectrum of the gamma rays from the ^{60}Co source to energy spectrum of the gamma rays in coincidence with the beta particles.

The MCA was used to record energy spectra from the beta silicon detector, the Ge detector, and timing spectra from the TAC. The MCA histograms the input pulses by height into channel, recording the

number of counts for each channel. With a calibration source, the channels can be calibrated to energy and an energy spectrum can be obtained.

3.3 TAC Output and Calibration

The timing spectrum was obtained with the range on the TAC set to 400 ns shown in Figure 30.

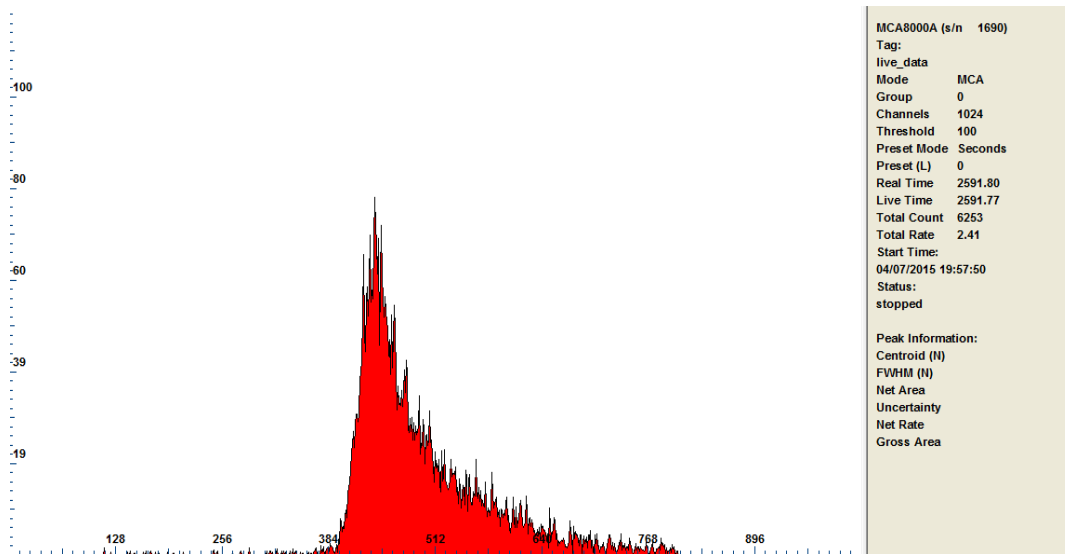


Figure 30: Un-calibrated timing spectrum. The TAC was set to a range of 400 ns. Full scale is at approximately channel 800 which is about 400 ns. The FWHM is therefore approximately 45 ns. Note, however, that there is a tail and that the timing spectrum is not Gaussian. This indicates that there are still a number of events that are at a much larger time difference apart.

According to these preliminary estimates, the TAC has a timing resolution of approximately 45 ns FWHM. The peak has been shifted to approximately the middle channel by delaying the signal from the Silicon surface barrier detector using the Gate & Delay Generator. With the peak shifted to the center of the spectrum, the timing spectrum can be calibrated by further delaying the stop signal on the TAC by a known amount using a linear delay. The difference in channels between both the initially centered peak and the further delayed peak can be used to calibrate the spectrum. With a known difference in

channels and a time difference, a function can be fit to determine the conversion of the channels to time in order to calibrate. The same process of channel calibration was applied to the histogrammed γ -ray energy spectrum shown in Figure 31. A rough estimate of the energy resolution was obtained from the spectrum of roughly 50 keV FWHM.

3.4 Analysis

A difference in the energy spectra for gamma rays in coincidence with the beta particles after the polarity of the magnet is changed, relative its initial polarity, is an indicator of parity violation. The γ -ray energy spectrum of ^{60}Co is shown in Figure 31.

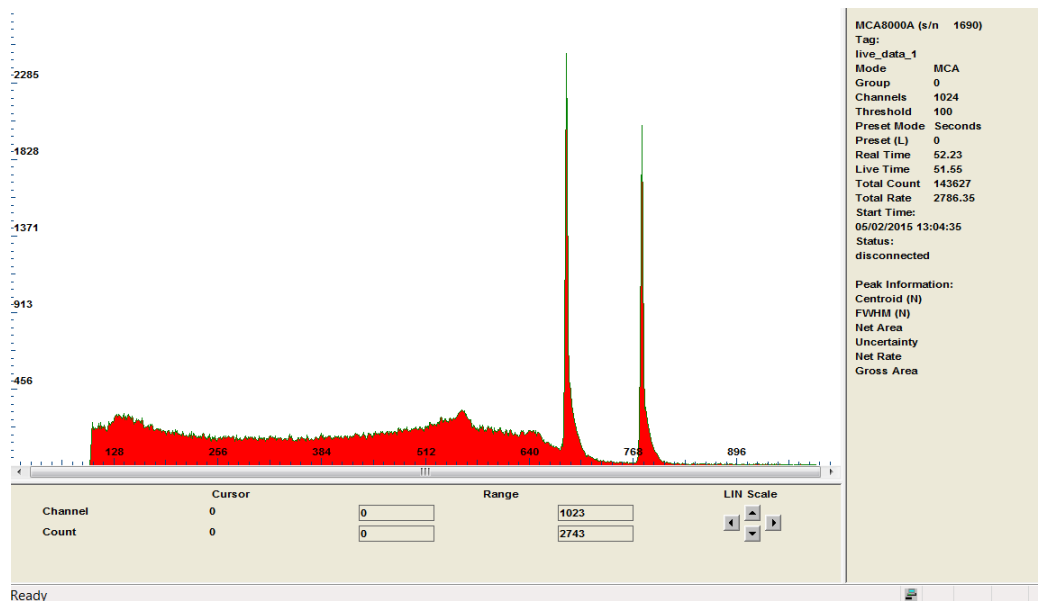


Figure 31: The γ -ray energy spectrum when the electromagnet is removed from the apparatus. The two peaks correspond to the 1.17 MeV and 1.33 MeV γ -rays shown in the ^{60}Co decay scheme in Figure 9. To determine which channel corresponded to γ -rays at each energy shown in the ^{60}Co decay scheme, an arbitrarily small range of channels surrounding each peak were selected. A weighted average was taken of all of the channels within each range surrounding each peak. This weighted average of channels corresponded to the γ -rays at known energies of 1.17 MeV and 1.33 MeV.

Note, however, that the γ -ray energy spectrum in Figure 31 was not measured in coincidence with the detected electrons, but, instead, independent of the electron detection. To determine the count rate of the 1.17 MeV and the 1.33 MeV γ -rays, the channel of each peak is first determined. This is done by selecting a range of channels wide enough to enclose just a single energy peak in the spectrum. From this, the weighted mean of those selected channels can be determined. The weighted mean of those selected channels is the channel that corresponds to a known energy in the ^{60}Co decay spectrum. From this a calibration from channels to MeV can be made. With the energy spectrum calibrated, the count rates of transmitted γ -rays of each polarity of the magnet can be compared from the difference in count rates of the γ -rays between each polarity of the magnetic field. This can be done by subtracting one spectrum from the other where the area of the reduced peaks gives the asymmetry. A difference in these count rates outside the statistical uncertainty, which is simply the \sqrt{N} , where N is the number of γ -rays counted for a particular energy, is an indication of parity violation.

3.5 Experimental Difficulties

Among the difficulties was ensuring that the detectors, as well as the ^{60}Co source and magnet, were collinear with each other. Attempts to increase collinearity were made by using disks of acrylic on the top and the bottom of the electromagnet with the ^{60}Co placed inside a cylindrical divot in the center of the top acrylic disk in order to make the source collinear with the detectors directly above and below the disks. This was done so that the magnet would not move relative to the surface of the detector. Collinearity in this experiment is important as a lack of symmetry may lead to systematic asymmetry that could be mistaken for parity violation.

Additionally, switching the direction of the current sent through the electromagnet was not automated. Measurements were made for a set duration for each direction of the current and the current direction was reversed by reversing the leads of the electromagnet going into the power supply of the electromagnet. However, this may not necessarily saturate the magnet symmetrically because of hysteresis.

Chapter 4

RESULTS AND CONCLUSION

4.1 Discussion

While the transmitted γ -ray energy spectra have not been measured in coincidence with electron emission, the circuit is working as evidence of the timing and γ -ray energy spectra obtained from the circuit. The timing resolution was measured to be roughly 45 ns FWHM which is sufficient for the purpose of this experiment. The γ -ray energy spectrum, also, is as expected, with two peaks from the de-excitation of the ^{60}Ni produced by the beta decay of ^{60}Co . A rough calibration and approximation of the energy resolution was obtained of the γ -ray energy spectrum of roughly 50 keV FWHM.

4.2 Conclusion and Future Plans

While the experimental setup largely complete, only preliminary measurements of the timing spectrum and γ -ray transmission energy spectra, have been made. The data presented in this thesis are very preliminary and not fully analyzed. Furthermore, coincidence measurements of the γ -ray energy spectra have not been made of the degree of asymmetry in the γ -ray transmission. Future work will consist of making measurements of the transmitted γ -rays to statistical uncertainty of less than 5% in asymmetry. In addition, measurements of the TAC output and the magnetic field through the electromagnet were intended to only measure the timing resolution of the circuit and saturation of the electromagnet, respectively. The total length of time that the experiment would need to run for was estimated to be approximately 100 days in total for the current thickness of the electromagnet. A 10 day collection period of the transmission of γ -rays through the electromagnet will only achieve a relative uncertainty in the asymmetry of approximately 15%. However, as shown in Figure 15, the uncertainty in the asymmetry can be reduced greatly by decreasing the thickness of the electromagnet or by housing the ^{60}Co source inside an axially symmetric, drilled cavity within the electromagnet to reduce the thickness of the material that γ -rays incident the Ge detector will have transmitted through. By doing so, the collection time

required for the relative uncertainty in the asymmetry to reach approximately 5% can be obtained in a much shorter time span.

In order to ensure that the same magnitude of current is sent through the electromagnet for each polarity and for the same amount of time, a circuit to automate the reversal of the current polarity at set, random time intervals should be constructed. Random time intervals are selected to eliminate possible systematic errors in asymmetry due to any time dependences that may exist. Currently, the reversal of current through the electromagnet is being done manually. This could lead to one orientation of the magnet being measured for longer than another orientation during the switching process of the current polarity or that. Additionally, it does not ensure that the current through the magnet is the same in the opposite direction which means that an orientation of the magnet may have a slightly different magnetic field, also introducing asymmetry in the measurement. There may also be affects that are dependent on the time of day, temperature, humidity, background radiation, and other possible contributions to the asymmetry that will need to be accounted for. Also, to improve axial symmetry, the experiment is intended to be repeated with the electromagnet rotated around its central axis.

References

1. Nobel Lectures, *Physics 1942-1962*, (Elsevier Publishing Company, Amsterdam, 1964).
2. T. D. Lee and C. N. Yang, *Phys. Rev.* **105**, 254 (1956).
3. M. Gardner, *The New Ambidextrous Universe: Symmetry and Asymmetry from Mirror Reflections to Supersymmetry*, 3rd Ed. (Dover Publications, Mineola, NY, 2005), pp. 212-213.
4. Ralph P. Hudson. *A Century of Excellence in Measurements, Standards, and Technology*, (NIST, Washington, DC, 2001), pp. 114.
5. E. P. Charles, *No Time to be Brief: A Scientific Biography of Wolfgang Pauli.*, (Oxford University Press, Oxford, 2002), pp. 520.
6. E. Rutherford, F. Soddy, *Phil. Mag.* **IV**, 370-96, 569-85 (1902).
7. Kasimir Fajans, *Berichte der Deutschen Chemischen Gesellschaft*, **46**, 422–439 (1913).
9. Ellis and Wooster, *Proc. R. Soc. Lond. A.* **117**, 109-123 (1927).
10. F. A. Scott, *Phys. Rev.* **48**, 391 (1935).
11. André Michaudon, *Phys. Today* **31**, 23 (1978).
12. E. Fermi, private letter to F. Reines (unpublished).
13. Fred Reines and Clyde Cowan Jr., *Los Alamos Science* **25**, (1997).
14. M. Goldhaber, L. Grodzins, and A. W. Sunyar, *Phys. Rev.* **106**, 826 (1957).
15. C. S. Wu, *Phys. Rev.* **105**, 1413 (1957).
16. R. L. Garwin, L. M. Lederman, M. Weinrich, *Phys. Rev.* **105**, 1415 (1957).
17. H. Schopper, *Phil. Mag.* **2**, 710 (1957).
18. Wigner, E.P. *Nachrichten von der Gesellschaft der Wissenschaften zu Göttingen, (Mathematisch Physikalische Klasse, 1927)*, pp. 375–381.
19. H. Schopper, *Nucl. Instrum.* **3**, 158 (1958).
20. O. Klein and T. Nishina, *Zeit. f. Phys.*, **52**, 853-868 (1929).
21. E. Browne and J. K. Tuli, *Nuclear Data Sheets* 114, 1849 (2013).